

See discussions, stats, and author profiles for this publication at: <https://www.researchgate.net/publication/342693500>

Development of a Membrane Filtration Cascade for the Recovery of Biomass-Derived Medium-Chain Fatty Acids

Thesis · July 2020

CITATION

1

READS

187

1 author:



Stewart Charles McDowall
Leiden University

4 PUBLICATIONS 13 CITATIONS

SEE PROFILE



UNIVERSITÄT
LEIPZIG



Development of a Membrane Filtration Cascade for the Recovery of Biomass-Derived Medium-Chained Fatty Acids

Master Arbeit

zur Erlangung des Grades
Master of Science (Chemie)

vorgelegt von

Stewart Charles McDowall, B. Sc.

Geboren: 07.07.1989 in Dubbo, Australien

Juni 2020

Betreut von

Roy Nitzsche, Dipl. Ing & Maria Braune, M. Sc.

DBFZ

Deutsches Biomasseforschungszentrum gemeinnützige GmbH

Bereich Bioraffinerien

&

Prof. Dr. Dirk Enke

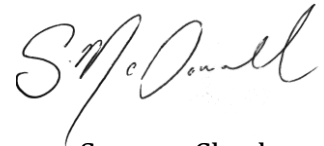
Universität Leipzig

Institut für Technische Chemie

Eidesstattliche Erklärung

Ich, der Unterzeichnende, erkläre hiermit an Eides statt, dass ich die vorliegende Arbeit selbständig verfasst habe und keine anderen als die angegebenen Quellen und Hilfsmittel benutzt habe. Alle Quellenangaben und Zitate sind richtig und vollständig wiedergegeben und in den jeweiligen Kapiteln und im Literaturverzeichnis wiedergegeben. Die vorliegende Arbeit wurde nicht in dieser oder einer ähnlichen Form ganz oder in Teilen zur Erlangung eines akademischen Abschlussgrades oder einer anderen Prüfungsleistung eingereicht. Mir ist bekannt, dass falsche Angaben im Zusammenhang mit dieser Erklärung strafrechtlich verfolgt werden können.

Brisbane, Australien 02.09.2020

A handwritten signature in black ink, appearing to read 'S. McDowall', written in a cursive style.

Stewart Charles

McDowall

Abstract

In this study, a separation cascade was developed for the recovery of medium-chained fatty acids (MCFAs) from fermentation broth (FB) using membrane technologies. The MCFAs were produced by the fermentation of maize silage in a mixed-culture chain-elongation process. The separation cascade consists of a basket press for solid-liquid separation, ultrafiltration (UF) for the removal of suspended solids and macromolecules, and nanofiltration (NF) to concentrate the MCFAs. Two ceramic UF membranes and three polymeric flat-sheet NF membranes were trialled in a technical-scale crossflow filtration. Investigations to establish the ideal process conditions were based on yield, flux and energy expenditure and included: thermal pretreatment, filtration parameter studies, UF and NF membrane screening, diafiltration, and membrane fouling analysis. In UF, permeate fluxes of $>50 \text{ kg m}^{-2} \text{ h}^{-1}$ and volume reductions of ~ 0.9 were achieved. Pretreatment and membrane pore size had no considerable influence on permeate flux and the limiting factor was concluded to be the formation of a cake layer on the membrane surface. In NF, volume reductions of >0.6 were attained, and the Tricep TS80 membrane had the highest MCFA retentions ($>90\%$). Although initial NF permeate fluxes with this membrane were high ($60\text{--}80 \text{ kg m}^{-2} \text{ h}^{-1}$), flux decline due to membrane fouling occurred rapidly, and near-total blockage limited the final concentration of MCFAs. While direct industrial application is restricted by the inadequate MCFA concentration, characterisation and reduction of NF membrane foulants could make this process viable. As it stands, this membrane filtration cascade provides an improved feedstock for the final purification of MCFAs by extraction or distillation.

Table of Contents

| | | |
|------|--|----|
| I. | List of Figures..... | II |
| II. | List of Tables..... | IV |
| III. | List of Abbreviations..... | V |
| IV. | List of Symbols..... | VI |
| 1. | Introduction..... | 1 |
| 2. | State of the Art..... | 3 |
| 2.1 | Fatty Acids | 3 |
| 2.2 | Recovery Methods for Medium Chain Fatty Acids | 5 |
| 2.3 | The Recovery of Organic Acids by Membrane Filtration | 6 |
| 2.4 | Fundamentals of Membrane Filtration..... | 8 |
| 3. | Materials and Methods | 17 |
| 3.1 | Experimental Overview..... | 17 |
| 3.2 | Maize Silage Fermentation Broth..... | 19 |
| 3.3 | Filter Press..... | 19 |
| 3.4 | Thermal Treatment | 20 |
| 3.5 | Membrane Filtration..... | 20 |
| 3.6 | Chemical and Physical Analysis..... | 30 |
| 4. | Results and Discussion | 32 |
| 4.1 | Basket Press Filtration..... | 32 |
| 4.2 | Thermal Treatment | 33 |
| 4.3 | Membrane Filtration - Sequence One | 34 |
| 4.4 | Membrane Filtration - Sequence Two..... | 41 |
| 4.5 | Fouling Analysis..... | 49 |
| 5. | Conclusion and Outlook | 58 |
| 6. | References..... | 61 |
| 7. | Appendices | 77 |

I. List of Figures

| | |
|--|----|
| Figure 2.1: The medium-chain fatty acids hexanoic acid and octanoic acid | 3 |
| Figure 2.2: The biochemical cycle of fatty acid chain elongation (48)..... | 4 |
| Figure 2.3: The separation pyramid of membrane filtration (18) | 8 |
| Figure 2.4: Rejection profiles showing the MWCO of two UF membranes (76)..... | 9 |
| Figure 2.5: An illustration of internal membrane fouling (89)..... | 12 |
| Figure 2.6: A theoretical filtration showing a typical flux decline over time (88) .. | 12 |
| Figure 2.7: Concentration polarisation. | 14 |
| Figure 2.8: The possible stages in cake layer formation during filtration (86)..... | 15 |
| Figure 3.1: An overview of the first experimental sequence | 17 |
| Figure 3.2: An overview of the second experimental sequence..... | 18 |
| Figure 3.3: Grifo PEW 20 basket press fitted with a canvas filter cloth | 19 |
| Figure 3.4: The PiloMemI membrane filtration apparatus..... | 21 |
| Figure 3.5: Process and instrumentation diagram for the PilomemI unit | 22 |
| Figure 3.6: The Alfa Laval LabStak M20 membrane filtration assembly..... | 23 |
| Figure 4.1: The feed, filtrate, and filter cake of the basket press filtration..... | 32 |
| Figure 4.2: The filtered FB before and after thermal treatment..... | 33 |
| Figure 4.3: Experimental determination of the critical flux..... | 34 |
| Figure 4.4: Permeate flux vs. volume reduction (VR) for UF in concentration mode of 86.6 kg of thermally treated FB on a 15 kD ceramic membrane..... | 35 |
| Figure 4.5: The ultrafiltration permeate and retentate | 36 |
| Figure 4.6: Permeate flux vs. transmembrane pressure (TMP) for the NF membranes ETNA01, NP030, and TS80 in total recirculation mode..... | 37 |
| Figure 4.7: Permeate flux vs. crossflow velocity (CFV) for the NF membranes ETNA01, NP030, and TS80 in total recirculation mode..... | 38 |
| Figure 4.8: Rejection coefficients for the C2-C8 fatty acids (FA) as a function of TMP for the nanofiltration (NF) membranes ETNA01, NP030, and TS80 | 40 |
| Figure 4.9: Permeate flux vs. volume reduction (VR) for the crossflow ultrafiltration (UF) of pressed maize silage fermentation broth (FB). | 42 |
| Figure 4.10: Permeate flux vs. volume reduction (VR) for the crossflow nanofiltration of ultrafiltration (UF) permeate from pressed maize silage fermentation broth (FB).. | 45 |

| | |
|--|----|
| Figure 4.11: Photographs of the typical NF retentate and permeate from the concentration of UF permeate from maize silage FB with a TS80 membrane | 47 |
| Figure 4.12: Permeate flux vs. VR for the diafiltration of UF (15 kD) permeate..... | 47 |
| Figure 4.13: Titration curve of the NF retentate with the addition of H_2SO_4 | 49 |
| Figure 4.14: PWF vs. TMP of the 15 kD ZrO_2 membrane. | 51 |
| Figure 4.15: PWF vs TMP of the 150 kD ZrO_2 membrane..... | 51 |
| Figure 4.16: A comparison of the pure water flux of the nanofiltration (NF) membranes ETNA01, NP030 and TS80 over two filtration and cleaning cycles..... | 53 |
| Figure 4.17: The pure water flux (PWF) for the two TS80 membranes over the concentration experiments | 55 |
| Figure 4.18: Photographs of the precipitates and residues found in the NF filtration streams..... | 56 |

II. List of Tables

| | |
|---|----|
| Table 3.1: NF Membrane Properties..... | 24 |
| Table 3.2: UF process parameters | 25 |
| Table 3.3: NF Concentration Experiment Process Parameters | 26 |
| Table 3.4: GC analysis parameters..... | 30 |
| Table 4.1 A partial mass balance of the basket press filtration..... | 33 |
| Table 4.2: Permeability of the NF membranes as a function of TMP..... | 37 |
| Table 4.3: Average FA concentration (C2-C8) and retention coefficients for the UF of maize silage FB at a volume reduction of ~ 0.9 | 43 |
| Table 4.4: Rejection coefficients with respect to C2-C8 FAs for the NF membrane TS80 in the concentration experiments (Exp. 2.6-2.10 & 3.1) | 45 |
| Table 4.5: Average fatty acid (FA) concentration (C2-C8) and retention coefficient for the NF of UF permeate from maize silage FB | 46 |
| Table 4.6: FA concentration and retention coefficient for the diafiltration (DF) during the NF of UF permeate from maize silage FB. | 48 |
| Table 4.7: The pure water permeability, flux recovery, fouling contributions and MgSO_4 retention for the 15 kD ZrO_2 UF membrane..... | 50 |
| Table 4.8: The pure water permeability, flux recovery, fouling contributions and MgSO_4 retention for the 150 kD ZrO_2 UF membrane | 50 |
| Table 4.9: A comparison of the average pure water permeability and MgSO_4 retention for the NF membranes ETNA01, NP030 and TS80 | 53 |
| Table 4.10: The pure water permeability, flux recovery, fouling contributions and MgSO_4 retention for the TS80 over the five concentration experiments | 54 |
| Table 7.1: Physical and chemical data of each stream in the study..... | 77 |
| Table 7.2: FA (C2-C8) concentration for each stream in the study | 78 |
| Table 7.3: Rejection coefficients with respect to the C2-C8 fatty acids for the ultrafiltration concentration experiments (Exp. 1.3 & 2.3-2.6) | 79 |
| Table 7.4: Rejection coefficients with respect to the C2-C8 fatty acids for the NF membranes ETNA01, NP030, and TS80 | 79 |

III. List of Abbreviations

| | |
|----------------|---|
| CE | Chain Elongation |
| CF | Concentration Factor |
| CFV | Crossflow Velocity |
| COD | Chemical Oxygen Demand |
| DBFZ | Deutsches Biomasseforschungszentrum [German Biomass Research Centre] |
| DF | Diafiltration |
| FA | Fatty Acid |
| FB | Fermentation Broth |
| GC | Gas Chromatography |
| ICP-OES | Inductively Coupled Plasma – Optical Emission Spectroscopy |
| MCCE | Mixed-Culture Chain Elongation |
| MCFA | Medium Chain Fatty Acid |
| MF | Microfiltration |
| MW | Molecular Weight |
| MWCO | Molecular Weight Cut-off |
| NF | Nanofiltration |
| PWF | Pure Water Flux |
| RO | Reverse Osmosis |
| RPM | Revolutions Per Minute |
| TMP | Transmembrane Pressure |
| UF | Ultrafiltration |
| UFZ | Helmholz Umweltforschungszentrum [Helmholtz Center for Environmental Research] |
| VFA | Volatile Fatty Acid |
| VR | Volume Reduction |

IV. List of Symbols

| Symbol | Unit | Description |
|---------------|--|-----------------------------|
| A | m^2 | Area |
| C | M | Concentration |
| d | nm | Apparent Molecular Diameter |
| d_p | m | Pore Diameter |
| k | - | Permeability Coefficient |
| k_w | $\text{m s}^{-2} \text{bar}^{-1}$ | Hydraulic Permeability |
| m | g | Mass |
| MW | D or g mol^{-1} | Molecular Weight |
| n | mol | Amount of Substance |
| P | bar | Pressure |
| ΔP | bar | Transmembrane Pressure |
| Q | $\text{m}^3 \text{s}^{-1}$ | Volumetric flow rate |
| q | $\text{m}^3 \text{m}^{-2} \text{s}^{-1}$ | Volumetric flux |
| q_w | $\text{m}^3 \text{m}^{-2} \text{s}^{-1}$ | Pure Water Flux |
| R | $\text{kg m}^{-4} \text{s}^{-1}$ | Resistance |
| RC | - | Rejection Coefficient |
| t | s | Time |
| T | $^{\circ}\text{C}$ | Temperature |
| V | m^3 | Volume |
| VR | - | Volume Reduction |
| w_{dr} | % (w/w) | Dry Residue |
| w_w | % (w/w) | Water Content |
| X | various | Driving Force |
| z | m | Membrane Thickness |
| μ | P s | Viscosity |
| ε | m^{-2} | Porosity |
| σ | mS | Electrical Conductivity |
| τ | - | Tortuosity |

1. Introduction

In the context of dwindling natural resources and an ever-expanding population, the traditional fossil-fuel-based linear economy cannot supply humanity's rapidly growing needs without simultaneously destroying our habitat (1). The imperative transition to a bio-based circular economy is gaining acceptance and has been formalised in research strategies and business plans from forward-thinking states and companies across the globe (2–7). The new bioeconomy will be based on an integrated system for the valorisation of renewable resources that maintains a synergy between ecological and economic principles (8–10). Just as the petrochemical refineries of today serve the old economic model, so must the biorefineries of tomorrow contribute to the foundations of the new, sustainable, circular economy (11).

In Germany, the development of integrated biorefineries has been gaining considerably in importance due to the impending expiration of biogas subsidies. Implementation of the Renewable Energy Sources Act in 2000 provided an economic incentive that has resulted in a seven-fold increase in the number of biogas plants, however, these subsidies have been reduced and are set to lapse in the coming years (12). While these 9000+ biogas facilities provide an important source of baseload electricity and account for more than half of the renewable energy production, low gas prices and reduced tariffs are predicted to make them rapidly uneconomical (13). The future of this sector, therefore, depends on diversification and value addition by coupling existing biogas facilities to biorefinery systems that can create a variety of more profitable products from biomass (14).

To this end, the co-production of medium-chain fatty acids (MCFAs) and gas from biomass has been identified as promising, and both the fermentation (upstream) and separation (downstream) processes are under intensive study (15). The MCFAs have the potential to become a new class of bio-based platform chemicals (16), and this study focusses on the development of a downstream biorefinery process for their recovery from fermentation broth (FB).

An efficient biorefinery must cheaply and sustainably convert biomass into energy and useful products, and an essential part of this is the fractionation of complex mixtures. Such downstream processes are currently responsible for a large proportion of the cost of bio-based products, though there is much scope for innovation and optimisation (10, 17–30). In particular, membrane filtration is considered a cost-effective and environmentally friendly separation technique, though long-term efficacy is often hindered by blocking of the filter pores (fouling). Process development, therefore, requires intensive and substrate-specific adaption and optimisation of pretreatment and operational parameters. Moreover, identification of appropriate membranes and suitable procedures for their maintenance adds further complexity to the system design.

This work aims to design an efficient membrane filtration cascade for the recovery of concentrated MCFAs from maize silage FB. The goal is to adapt and optimise an established and environmentally friendly separation technique for a new biorefinery application. The approach used in this study is to develop a filtration cascade by adapting proven technologies to achieve a liquid-solid separation, then to increase MCFA concentration by dewatering, thereby facilitating subsequent purification.

The main objectives of this study are to:

- achieve an efficient solid-liquid separation by implementing a two-step filtration process consisting of a filter press and ceramic UF;
- screen candidates to identify a NF membrane that can effectively concentrate the MCFAs by dewatering; and
- optimise the membrane filtration cascade by conducting pretreatment screening (thermal treatment & UF pore size), parameter studies (pressure, flowrate), diafiltration, and fouling analysis.

The application of membrane filtration to the selective recovery of products from unrefined, biomass-derived FB has not yet been extensively studied. It is hoped that this work can contribute not only to the development of this specific process, but that knowledge can also be gained which aids in the progress of the field of biorefining as a whole.

2. State of the Art

2.1 Fatty Acids

Fatty acids (FAs) are a class of naturally occurring mono-carboxylic acids that typically contain an unbranched aliphatic carbon chain with an even number of carbons between 4 and 28 (C4-C28). Of interest in this study are the C6 and C8 MCFAs, hexanoic and octanoic acid (Figure 2.1), and, to a lesser extent, the C4 volatile fatty acid (VFA) butanoic acid. These acids have numerous applications: either directly as a nutritional supplement for animals and humans or indirectly in the manufacture of products including flavours, fragrances, lubricants, pharmaceuticals and dyes (31). Harvey and Meylemans (2014), and Urban (2017) have also demonstrated the potential of hexanoic acid as the basis for the renewable production of jet and diesel fuels (32, 33). Given the strong demand growth for these acids and their relatively high market prices (C4: 2200, C6: 2200, C8: 3700 € ton⁻¹ [2019]) (34, 35), there are increasing efforts to find novel sources that are both environmentally sustainable and economically feasible (36–38).

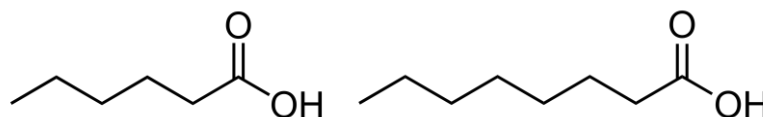


Figure 2.1: The medium-chain fatty acids (MCFAs) hexanoic acid (left) and octanoic acid (right) are also known as caproic acid and caprylic acid.

Presently, the C4-C8 FAs are mostly derived from non-sustainable resources. The current industrial-scale production of butanoic acid is from the oxidation of propene-derived butanal (39), and while bio-based butanoic acid can be extracted from butter, (~3% w/w), this process is prohibitively expensive (40). Hexanoic and octanoic acid can also be synthesised from petroleum feedstocks but they are mostly recovered by fractional distillation from the edible crops coconut (*Cocos nucifera*) and oil palm (*Elaeis guineensis*) (41–43) which places pressure on food prices and can harm the tropical environment (44).

Given the urgent need to reduce both our impact on the carbon cycle and our dependency on non-sustainable agricultural practices, it is imperative that alternative processes are established (45, 46). To this end, a microbial biochemical process called chain elongation (CE) is being developed which can produce FAs from biomass. This process consists of two main stages by which the organic macro-molecules are first broken up into smaller (C1-C2) fragments before being recombined by CE to larger molecules ($\geq C4$) (47). More specifically, in the CE stage, a bacterium sequentially elongates carboxylic acids by using ethanol, acetate, or lactate as an electron donor, and as a source of carbon and energy (Figure 2.2) (31, 48–51).

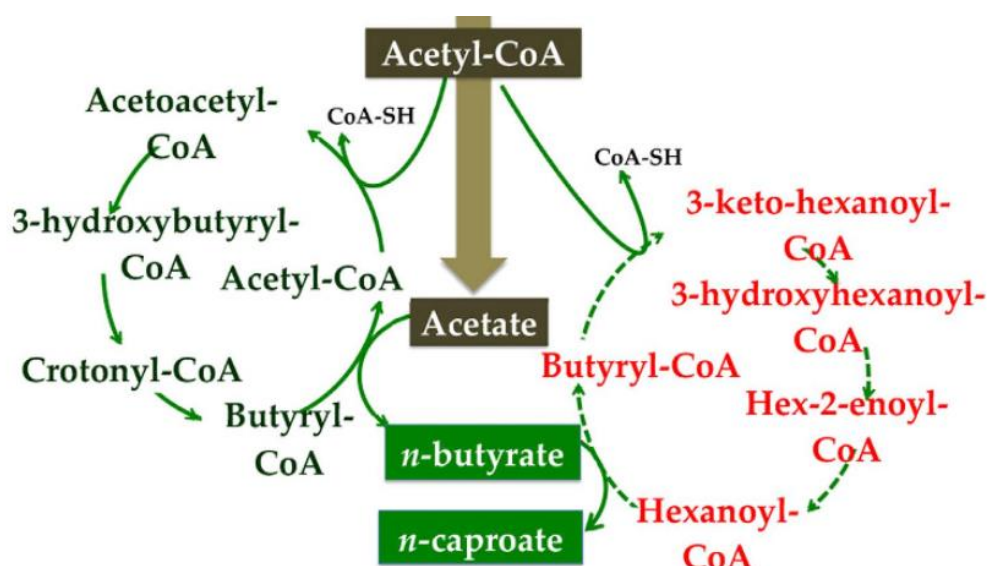


Figure 2.2: The biochemical cycle of fatty acid chain elongation (50)

To obtain acceptable yields of C4-C8 FAs, however, it is essential that tight process control is maintained, and that methanogenic organisms are suppressed so that the products are not consumed (16). A further yield limitation is that the CE products are toxic to the organisms that make them, and since long-chain FAs are essential to cell function it is not possible to completely suppress their synthetic pathways in favour of shorter-chained FAs (52). While this has presented significant challenges, and although the underlying microbial pathways are not yet completely understood (31), CE fermentations have been able to be broadened to function with

a variety of feedstocks and microorganisms in an improved process called mixed-culture chain elongation (MCCE) (52–57). While pure-culture CE is easier to control and can result in higher FA concentrations ($>30 \text{ g L}^{-1}$), only MCCE has potential as a platform production technology because it can continuously and stably operate with diverse, non-sterile feedstocks (16).

A proprietary process of this kind has been developed to convert organic waste into MCFAs at a pilot-plant scale by Chaincraft B.V (The Netherlands) (58) and is currently undergoing regulatory review (59). The drawback of the Chaincraft process, however, is that it requires the costly addition of externally sourced ethanol (47). The source of FAs for this study was the fermentation of maize silage in an MCCE process established at the Helmholtz Centre for Environmental Research (UFZ, Germany) (60). One advantage of this process is that the maize silage has a high concentration of lactic acid that can be used by bacteria as an energy and carbon source for CE, thus avoiding the need for external ethanol. However, like other MCCE production processes for MCFAs, the combined maximal concentration in the FB is typically limited to $\sim 10 \text{ g L}^{-1}$, a fact which makes downstream processing both challenging and potentially expensive (16).

2.2 Recovery Methods for Medium Chain Fatty Acids

To develop an MCFA production process suitable for integration into a biorefinery it is essential to establish a method of product recovery that is environmentally friendly as well as energy- and cost-efficient (45). While numerous studies have reported full or partial recovery processes for biomass-derived MCFAs, none have yet been proven to be both efficient and scalable (16, 49, 55).

The recovery of MCFAs can be achieved either directly from the bioreactor during fermentation, or by batch-wise treatment of the fermentation broth. Direct extraction has the advantage that product-inhibition effects on the bacteria are minimised by preventing the FA concentration from reaching toxic levels (49). However, this presents additional challenges as the separation process must operate in conjunction with and not inhibit the sensitive biosynthesis in MCCE. An

early example of direct extraction is the in situ biphasic reactive extraction of FAs using trialkyl phosphates and has been reported with many solvents including fatty alcohols (61–63), aromatics (64), or kerosene (62). While MCFA concentrations of up to 32 g L⁻¹ were achieved, these studies were limited in scale (<1 L) and often used expensive or hazardous solvents. More recent studies have used pertraction (membrane aided extraction) with a mineral oil, thereby avoiding contact between the extractors and the biomass (56, 65, 66). A promising approach, using a combination of in-line pertraction and membrane electrolysis, exploits the low solubility of associated C6 and C8 FAs (10.82 g L⁻¹ and 0.68 g L⁻¹) and pH control to continuously produce an oil containing 53% hexanoic acid and 37% octanoic acid (67). This system, based on a liquid by-product of the corn-to-ethanol industry, is being intensively developed, and while proven to be moderately stable and effective, it remains complex and energy-intensive. A further limitation of this process is that it would likely require additional solid-liquid separation steps to handle other types of biomass, which often have a much higher solids loading. Overall, despite some positive results in the previously described MCFA recovery studies, the scalability and economic viability of these processes is yet to be confirmed and further development is necessary (49).

2.3 The Recovery of Organic Acids by Membrane Filtration

The selective and efficient separation of organic acids from FB requires the adaption and optimisation of the process to minimise problems such as membrane fouling and product loss. While no studies have been published concerning the successful recovery of concentrated MCFAs from FB with pressure-driven membrane filtration, lessons can be taken from similar processes with other low molecular weight (MW) carboxylic acids.

A variety of multi-step recovery methods have been reported for bio-based succinic acid and lactic acid, often including an MF step for FB clarification followed by NF for purification and reverse osmosis (RO) for concentration by dewatering (68–71). These methods are yet to be proven at scale and despite an efficient biosynthesis of the acids, their separation accounts for more than 50% of costs and

is still considered a bottleneck in production (72, 73). Indeed, Lopez (2014) argues that, due to interference by salts such as sulphate, NF and RO processes do not appear to be an ideal method of purification for products such as lactic acid and butanoic acid from FB (74).

While VFAs such as butanoic acid are the most similar compounds to the MCFAs in terms of functionalisation and acidity, their shorter carbon chains mean they are smaller and more polar which will likely lead to considerable retention differences during NF. The multifaceted transport mechanism in NF makes the retention behaviour of membranes difficult to predict, though it has been found that hydrophobicity and a high negative surface charge favour the rejection of butanoic acid (75). The retention of VFAs by NF increases with high pH due to charge repulsion effects, though size exclusion is also a factor, as differences have been reported between the rejection of C2 and C4 FAs (76). In one study with biogas hydrolysate, FAs \geq C4 were concentrated up to a factor of 19 with several NF and RO membranes, though this was with a dead-end stirred-cell filtration unit (77). Pretreatment of the feed by UF (10-50 kD) was shown here to reduce fouling and increase the flux in the subsequent filtrations with complete transmission of the FAs.

With careful selection of the membranes and process conditions, it is, therefore, possible to direct the FAs to the desired filtration stream and even to fractionate the FAs based on size (25). With negatively charged membranes at a pH >6 the majority of the FAs will remain in the NF retentate. By using a lower pH or a positively charged membrane the acids can easily permeate the NF filter and can be subsequently concentrated by RO (78).

While the studies mentioned in this chapter, as well as knowledge of the physicochemical interactions, can certainly aid in the design of a filtration cascade, there are critical gaps in the research. The effects of pretreatment, process parameters and membrane selection on flux, fouling and MCFA rejection remain largely unknown. A better understanding of these processes gained through screening a variety of factors is crucial to the development of an efficient and scalable process for the recovery of MCFAs from FB.

2.4 Fundamentals of Membrane Filtration

Membrane filtration processes rely on selective transport across a semipermeable barrier and can be loosely categorized by membrane pore size; microfiltration (MF) 0.1-10 μm , UF 10-100 nm, NF 1-10 nm and RO >1 nm (79). The membranes are usually made from polymers or ceramics (only MF and UF) and can be operated in either dead-end or crossflow modes. By combining multiple steps, a well-designed membrane filtration cascade can isolate any desired fraction from a mixture (Figure 2.3).

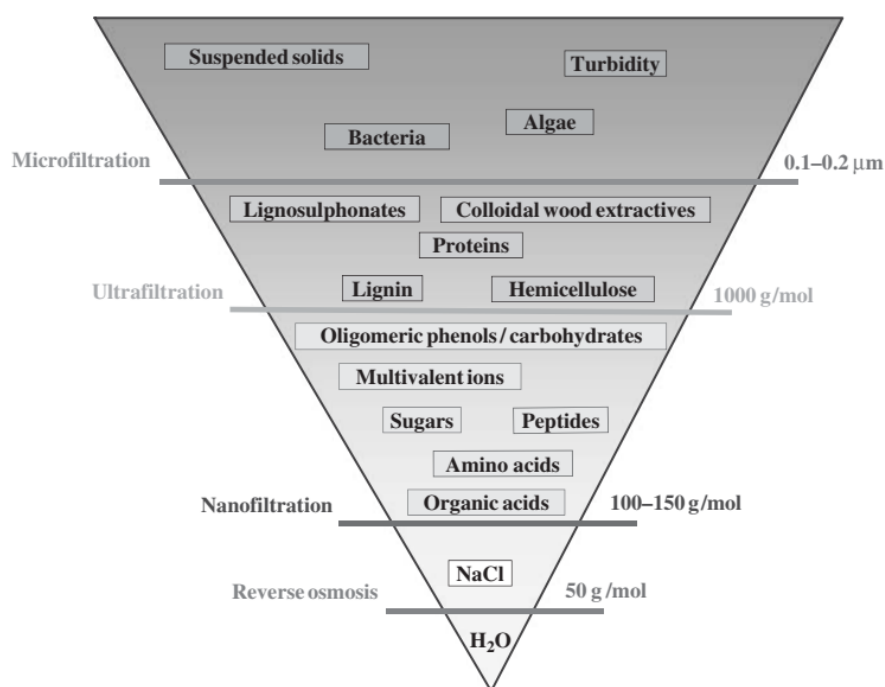


Figure 2.3: The separation pyramid of membrane filtration (19)

The separation of solutes and particles from the mixture results from differences in the permeability of the membrane with respect to each component. For UF, and NF, in which the pores are very small, the membranes are usually characterised by their molecular weight cut-off (MWCO), an experimentally determined value defined as the smallest MW of a molecule which will be retained to more than 90%. The MWCO can be determined as in Figure 2.4 by graphing the retention of a range of marker molecules. The steepness of the curve is inversely proportional to the width of the pore size distribution of the membrane. UF

membranes typically have an MWCO between 1000 D and 300 kDa while NF membranes have an MWCO of <1000 Da (79).

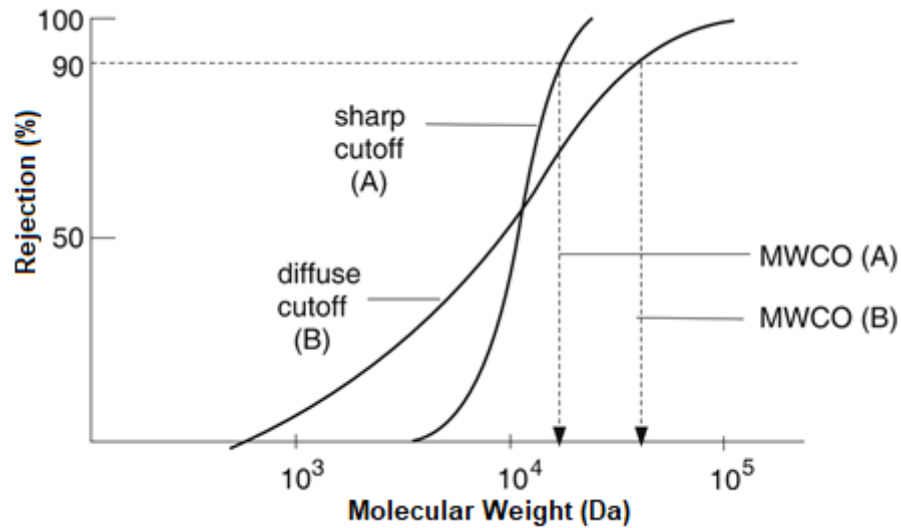


Figure 2.4: Rejection profiles showing the MWCO of two UF membranes (79)

The driving force for the mass transport across the membrane can be gradients in the chemical potential, electrical potential or hydrostatic pressure (80). The Darcy equation (Equation 2.1) describes the flux (q) of a component (i) across a porous membrane as a function of its permeability coefficient with respect to the membrane (k_i), the driving force (X_i), and the thickness of the membrane (z) (81)

$$q_i = \frac{k_i}{z} X_i \quad (2.1)$$

The UF and NF processes in this study are pressure-driven, so the main driving force of the separation is given by the hydrostatic pressure difference (ΔP), often called the trans-membrane pressure (TMP). Although the driving force is the same in both processes, charge effects are much more important in NF for determining solvent and solute permeability because the modes of mass transport differ.

2.4.1 Mass Transport in Ultrafiltration

The pore sizes in UF are large enough that the mass transport can be considered as convective flow and can be described by a modified version of the Hagen-Poiseuille model of capillary flow (Equation 2.2) (82)

$$q = \frac{\varepsilon \cdot d_p^2 \cdot \Delta P}{32 \cdot z \cdot \mu \cdot \tau} \quad (2.2)$$

where ε is the porosity d_p is the pore diameter, τ is the pore tortuosity and μ is the viscosity of the solvent. The means of separation in UF is predominantly a sieving effect whereby all solids and solutes larger than the pores of the membrane are retained. In this study, the purpose of the UF step in the membrane cascade is to remove these higher MW components from the FB to minimise flux decline during the NF step.

2.4.2 Mass Transport in Nanofiltration

The small size of the pores in NF means that it can be considered a partially dense membrane and, as such, the mass transport cannot be adequately described by capillary flow models (83). Mass transport through a completely dense material (such as an RO membrane) is determined by solution and diffusion processes which can be described simplistically by Fick's Law (84). A thorough and quantitative description of mass transport in NF is extremely complex for heterogeneous substrates and is outside the scope of this study (85). However, consideration of the electrical and chemical properties that control solution and diffusion is useful for understanding important relationships in filtration performance and membrane selectivity. For example, in comparison to UF, parameters such as pH, feed concentration, and membrane surface charge have been shown to have much greater effects on flux and solute rejection in NF (86, 87). Although the separation mechanism for uncharged molecules can still be governed by the sieving effect, for charged and polar species it is their electrical and chemical properties relative to those of the membrane which plays the dominant role in separation (19). Small molecules like MCFAs, for example, can be rejected by NF membranes with a much higher MWCO than their MW if the feed pH is such that both the membrane and the

acids are negatively charged (74). In this study, high rejections in NF are desired and are expected because the NF feed pH (~ 7) is greater than both the pKa of the FAs (~ 4.8) and the isoelectric points of the membranes (~ 4).

2.4.3 Challenges in Membrane Filtration: Fouling and Selectivity

While membrane filtration is an established industrial separation technique (79), its application to the purification of FB often presents serious challenges due to fouling on membrane surface caused by the substrate (88). FB is especially difficult to filter because it is a complex and often undefined mixture that include cells, extracellular polymeric substances (EPS), proteins, lipids, polysaccharides and salts. The transport models described above assume that the only resistance is that which is inherent to the membrane, thus they cannot adequately describe a filtration system which is, by definition, heterogeneous. The interaction of the feed components with the membrane leads inevitably to flux decline caused by increased resistance due to fouling mechanisms. The flux equation described above (Equation 2.1) can be modified for pressure-driven filtration by incorporating the TMP (ΔP) and viscosity (μ) and replacing the permeability term (k) with a resistance term (R_{tot}) which includes the hydraulic resistance (R_w) of the membrane and any additional resistance caused by the substrate (Equation 2.3)

$$q_i = \frac{\Delta P}{\mu \cdot R_{tot}} \quad (2.3)$$

By assuming a linear addition, the total resistance can be separated into its components by the resistance-in-series model of membrane fouling (82). A recent literature review listed more than 20 different (often overlapping) classifications of component and sub-component resistances (89). These component resistances can differ by nature (reversible/irreversible by cleaning/parameter variation), location (external/internal) and cause (solute/colloid/particle). The main additional component resistances are attributed to internal fouling (R_f), concentration polarisation (R_{CP}) and external cake layer formation (R_c), giving

$$R_{tot} = R_w + R_f + R_{CP} + R_c \quad (2.4)$$

The additional resistance caused by internal fouling is a result of pore-blocking and pore constriction. Pore blocking occurs when foulants larger than the pore size become lodged in the opening whereas pore constriction is caused by the absorption of smaller molecules to the pore channel which decreases the effective pore diameter (Figure 2.5) (90).

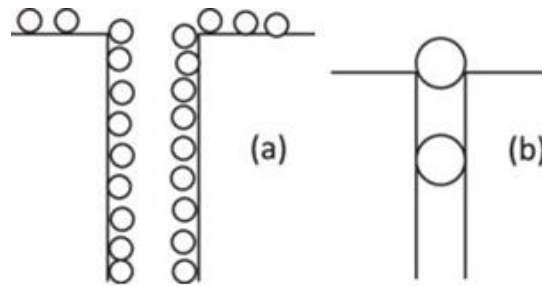


Figure 2.5: An illustration of internal membrane fouling due to (a) pore constriction by absorption and (b) pore blockage (91)

The component of internal fouling which can be removed by cleaning is categorised as (chemically) reversible fouling, while that which remains is referred to as irreversible fouling (Figure 2.6) (92). While flux decline due to reversible fouling can be more easily mitigated, avoidance or reduction of irreversible fouling more difficult, but is critical to the service life of a membrane.

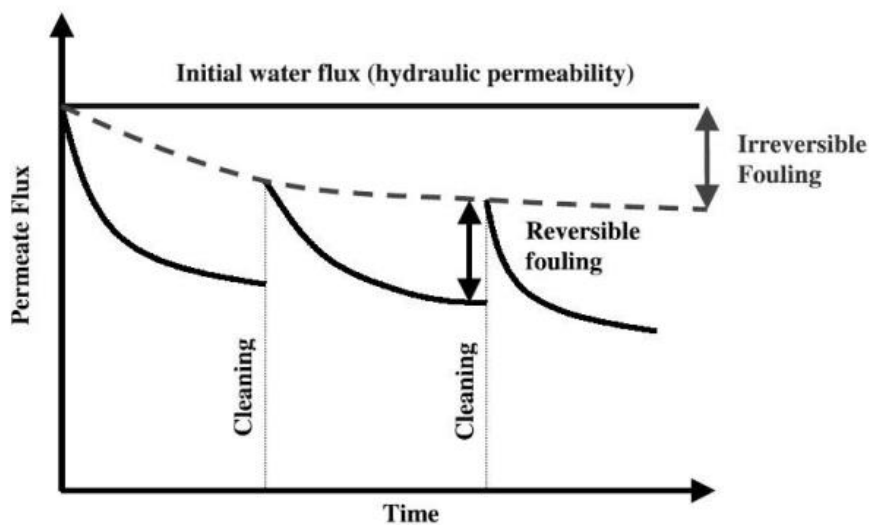


Figure 2.6: A theoretical filtration cycle showing a typical flux decline over time and the respective fouling components (92)

Another problem in membrane separation processes is the decline in membrane flux caused by concentration polarisation. This effect is inherent in nature of filtration and results from the accumulation of the less permeable and a depletion of the more permeable species. This additional resistance is proportional to permeate flux and occurs in the laminar boundary layer at the surface of the membrane due to a combination of selective transport and low bulk mixing. (81). At the membrane-solution interface, the velocity of the liquid approaches zero, convective mixing with the bulk region does not occur and the only form of mass transport is diffusion (93). While the rate of diffusion is proportional to the concentration gradient, this process is around two orders of magnitude slower than convective transport. The local concentration gradient causes an increase in osmotic pressure which leads to a decrease in effective pressure and thus a drop in membrane flux (81).

Additionally, if the concentration of a retained species at the membrane surface exceeds its solubility, it can form a gel layer which adds an additional hydrodynamic resistance to the membrane flux. This is especially the case for macromolecules such as proteins and polysaccharides, which have a low diffusion coefficient and limited solubility (82). Once the concentration at the membrane surface has reached the solubility limit, further increases in flow or applied pressure will lead to growth in the gel layer and a corresponding increase in resistance (Figure 2.7). The movement of foulants away from the membrane by shear- and Brownian-diffusion is then exceeded by their forward convection due to permeate drag forces and they will accumulate (94). Since the fouling and osmotic back-pressure are proportional to the permeate flow rate, a point of critical flux is reached where the transport across the membrane is no longer pressure dominated and the relationship between TMP and flux deviates from linearity (95). Further increases in TMP will lead to the point of limiting flux, above which flux does not increase and fouling is greatly accelerated (81, 82). While the obvious solution is to increase turbulence, this inevitably comes at the cost of energy efficiency. Knowledge of the critical/limiting-flux is important for the optimisation of membrane filtration processes so as to maximise throughput while minimizing energy waste and membrane fouling (96).

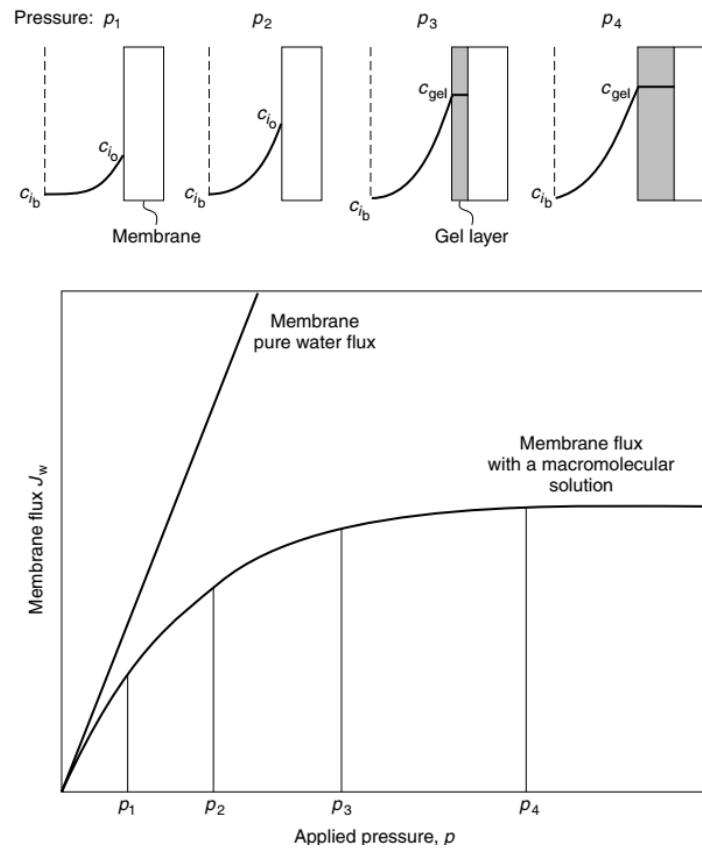


Figure 2.7: Concentration polarisation causes an increase in the concentration of macromolecule (i) at the membrane surface which leads to the formation of a gel layer and membrane fouling. The optimal TMP is situated between p_2 and p_3 where flux is high, but gel formation has not begun. (82).

Cake and Gel Layer Formation

External membrane fouling due to cake and gel layer formation adds an additional barrier to permeate flow and is mainly caused by membrane surface deposition of particles and macromolecules larger than the pores (81, 89). If the active foulants reach the membrane surface and adhere before the inert substances, a heterogeneous cake layer will form, thereby restricting flux through additional hydraulic resistance (97). Furthermore, the cake layer can contribute to enhanced concentration polarisation by adding an extra, unmixed surface layer where gel formation can occur. While this usually leads to additional overall resistance that is proportional to TMP (96, 98, 99), depending on the porosity of the cake layer and the feed constituents, it can also positively affect permeate flux by acting as a prefilter (Figure 2.8) (100, 101).

Depicted in the right-hand side of the figure, such a prefilter can develop if the larger, inert materials form a porous cake through which the solvent and solutes can pass freely while the foulants are restricted and prevented from adhering to the membrane surface (89).

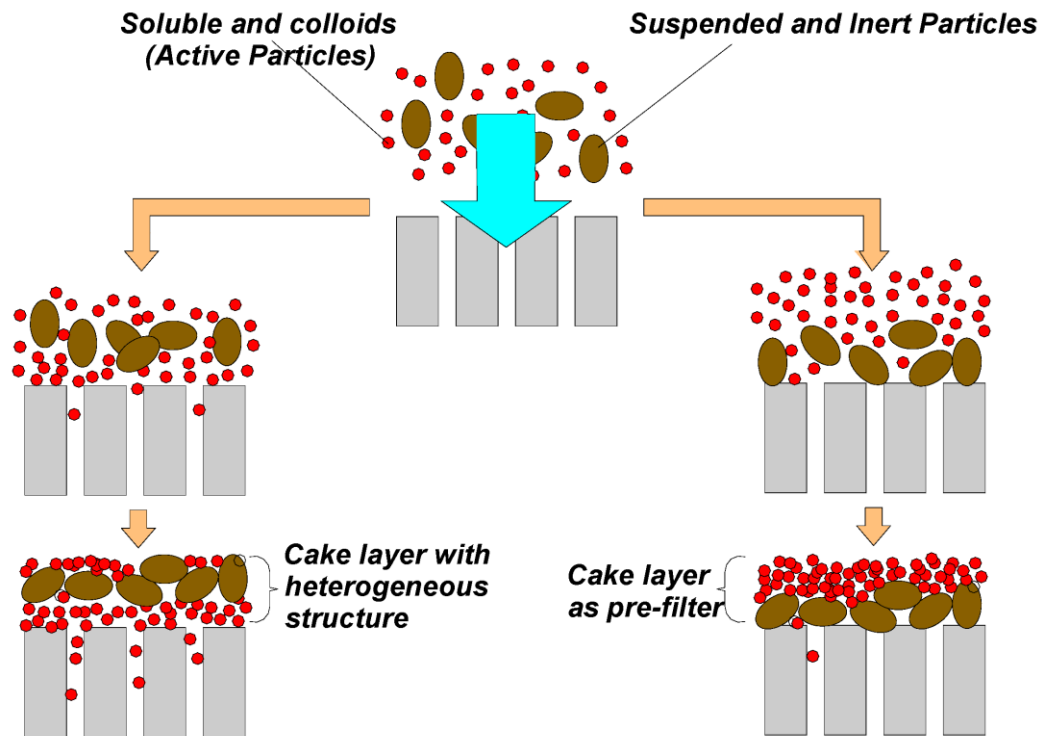


Figure 2.8: The possible stages in cake layer formation during filtration (89)

2.4.4 Controlling Membrane Fouling

Membrane fouling is an extremely complex physiochemical phenomenon and the development of control methods requires knowledge of the fouling agent, the fouling mechanism and the influence of the process parameters specific to the application (90, 68, 102). Several theoretical models have been developed for the determination of the dominant fouling mechanism based on flux decline data (19, 89), although their application to FB is, as yet, untested. By knowing which type of fouling has the greatest impact on flux decline and how it arises, the most appropriate and effective control measures can be implemented.

Internal fouling, for instance, has been found to be highly dependent on surface chemistry and could, therefore, be minimised by appropriate membrane selection and careful consideration of the potential substrate-membrane

interactions (e.g zeta potential, isoelectric point and hydrophobicity) (103, 104). The process parameters TMP and crossflow velocity (CFV) are of particular importance in fouling control as higher TMPs increase concentration polarisation and gel/cake layer development whereas the elevated CFVs can prevent this through enhanced turbulent convection (by decreasing the laminar boundary layer on the membrane surface) (105).

The pretreatment of membrane feeds is another possible way to control fouling and could include thermal treatment, pre-filtration, pH adjustment or enzyme digestion (19, 68, 106). Thermal treatment is often used to improve filtration performance in milk waste processing (107) and was trialled with the FB in this study. The flux decline which cannot be mitigated by fouling control can mostly be recovered by cleaning, though this can be costly and environmentally hazardous (94). Depending on the nature of the membrane and the foulant, this reversible fouling can be removed between filtration cycles. This is achieved either physically (backflushing/rinsing), or chemically, with acidic, basic, oxidative or enzymatic cleaning agents (82, 108). In this study, a relatively mild cleaning regime was performed (as per manufacturer recommendations), however, complete process optimisation would require detailed experiments to determine the best procedure which applies to the given substrate/membrane combination.

3. Materials and Methods

3.1 Experimental Overview

An overview of the experimental work is depicted in Figure 3.1 and Figure 3.2. In the first experimental sequence, thermal pretreatment and 15 kDa UF were performed prior to NF as these were expected to result in maximal permeate flux. Screening was then undertaken for the three NF membranes and the process parameters TMP and CFV. After selecting the optimal parameters and the best NF membrane based on flux and FA retention, pretreatment screening was conducted in the second experimental sequence. Here, the effects of thermal pretreatment, UF membrane pore size and diafiltration were tested with respect to NF flux and FA retention.

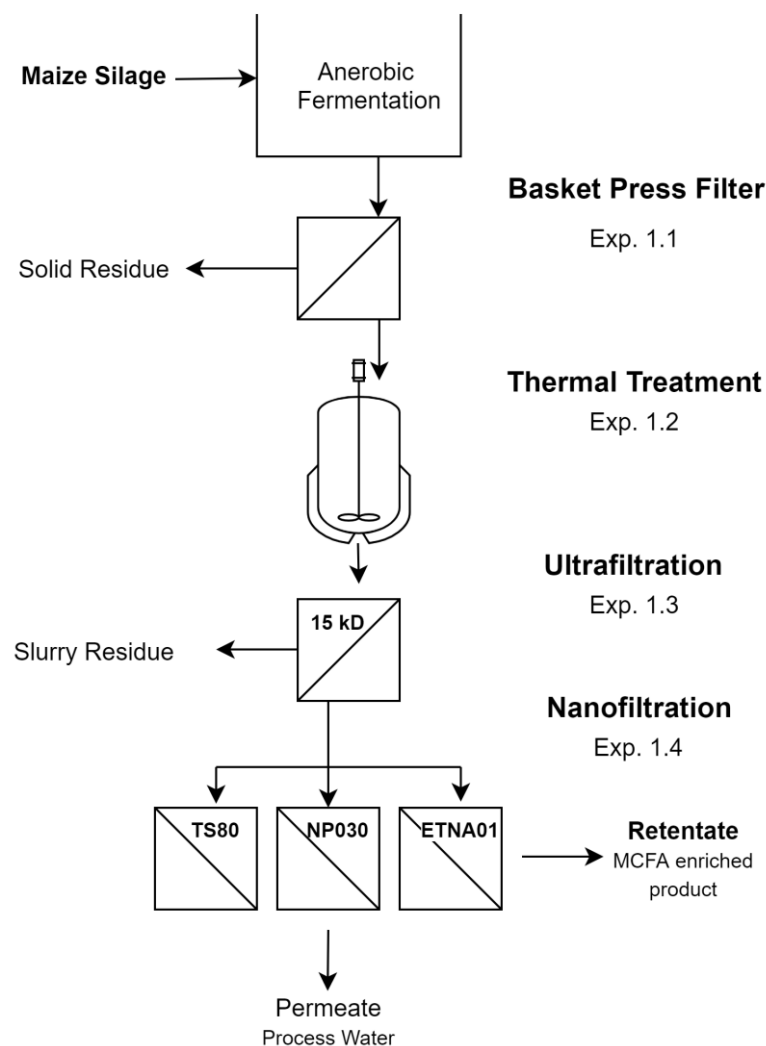


Figure 3.1: An overview of the parameter and nanofiltration membrane screening, the first experimental sequence

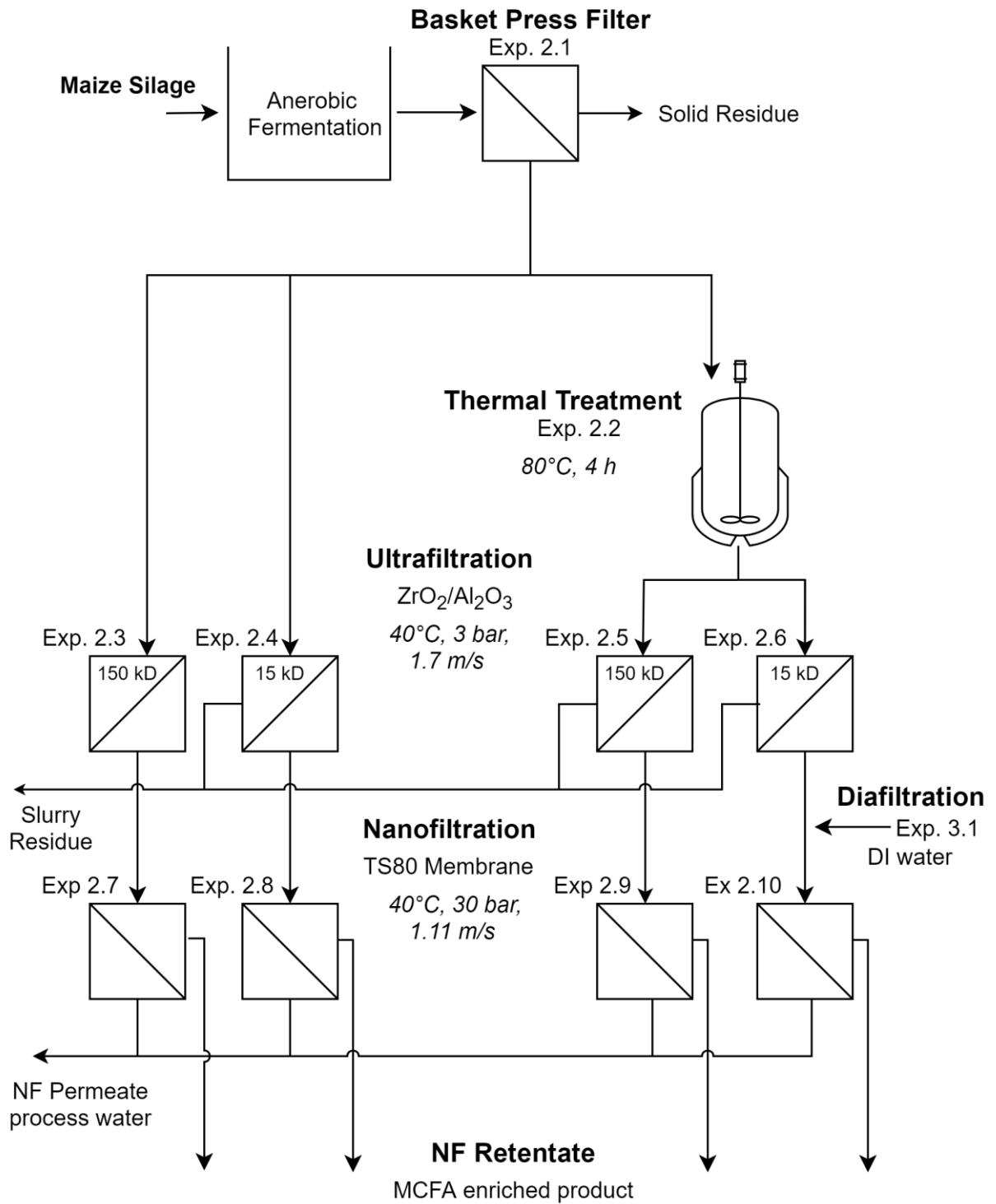


Figure 3.2: An overview of the second experimental sequence: screening of ultrafiltration membranes, pretreatments and diafiltration

3.2 Maize Silage Fermentation Broth

FB was obtained from experimental reactors at the DBFZ, supplied by a separate group. The maize silage was fermented by a mixed bacterial culture in a semi-continuous anaerobic process designed by the UFZ (60). The fermentation was supplemented daily with trace elements as well as urea (N source), and NaOH for pH control. The FB was removed periodically in 3-6 L batches from the 20 L reactors and stored at 4 °C.

3.3 Filter Press

To separate the coarse solids from the FB, the slurry from the reactors was filtered through a canvas cloth in a PEW20 pneumatic basket press from the manufacturer Grifo (Italy) (Figure 3.3). The FB was filtered at ~8 °C in 30 L batches under a pressure of 3 bar for around 30 min.

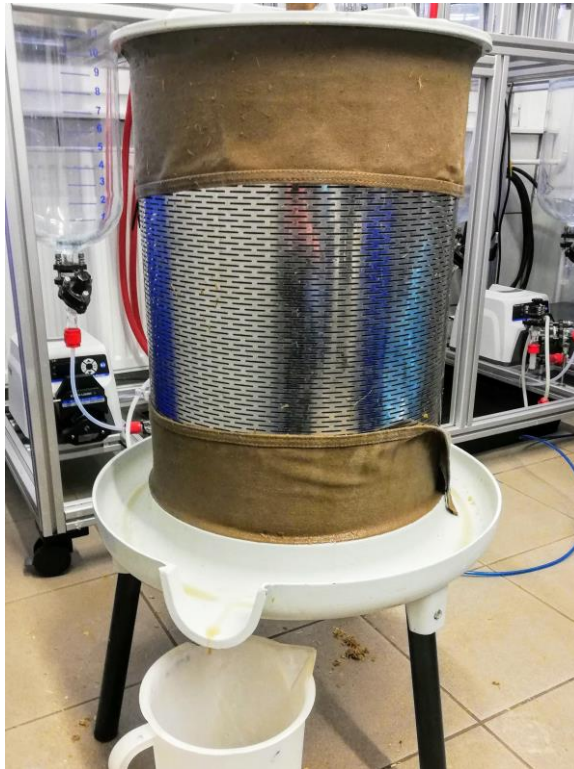


Figure 3.3: Grifo PEW 20 basket press fitted with a canvas filter cloth

3.4 Thermal Treatment

To investigate the effects of macromolecule denaturation on UF and NF performance, the basket press filtrate was heated in a custom-built, 130 L jacketed stainless steel reactor. During the first experimental sequence, 100 L of the FB was heated to a temperature of 90 °C over 8.5 h under mechanical stirring at 100 RPM. In the second experimental sequence, the heating time was only 3.5 h because the FB volume was 50 L and the heating power was constant. A briefer heating phase in a heat exchanger would have been ideal, but the equipment was not available. The FB was allowed to cool overnight before being transferred to 30 L plastic drums for storage at 4 °C.

3.5 Membrane Filtration

3.5.1 Materials

Ultrafiltration

UF processes were performed with a PiloMemI crossflow membrane filtration apparatus from PS Prozesstechnik GmbH (Switzerland) (Figure 3.4). The filtration unit was fitted with multi-channel tubular ceramic membranes from the manufacturer atech innovations (Germany). The two membranes were composed of a ZrO₂ active layer on an α -Al₂O₃ support, were 1178 mm long with seven 6 mm diameter channels and had a total surface area of 0.16 m² (109). The 15 kDa membrane had a pore size of approximately 400 nm, the 150 kDa membrane, 1200 nm.



Figure 3.4: The PiloMemI membrane filtration apparatus

The process and instrumentation diagram (PID) for the filtration unit is depicted in Figure 3.5. The FB in the temperature regulated feed tank (B01) was passed over the membrane (M01) and the retentate was returned to the tank through the heat exchanger (W01). Feed side pressure was regulated by adjusting the pump power (P01) and the post-column valve (V05). TMP was set by adjustment of the permeate-side valve (V08). In total recirculation mode, the permeate was returned directly to the feed tank, whereas in concentration mode it was collected in containers. Flow rate measurements from FIR02 were verified gravimetrically by periodically weighing the collected permeate.

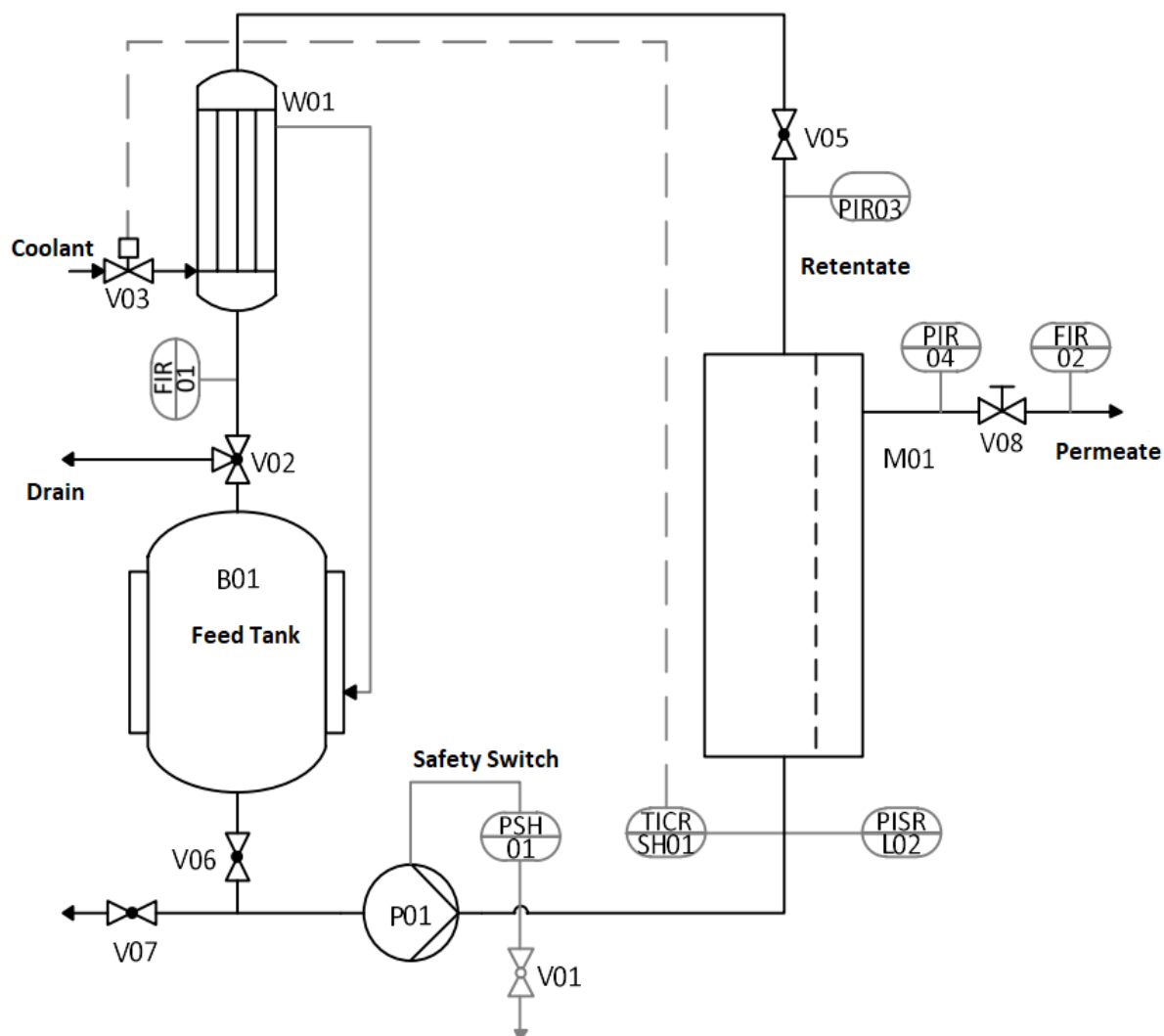


Figure 3.5: Process and instrumentation diagram for the PilomemI filtration unit

Nanofiltration

Crossflow NF experiments were performed with a LabStak M20 plate-and-frame membrane assembly from the manufacturer Alfa Laval (Denmark) (Figure 3.6). This filtration module was connected to the PiloMemI unit in place of the ceramic column and consisted of a stack of 20 cm flat sheet membranes within plastic plates held in a steel frame, secured by pressure from a piston pump.

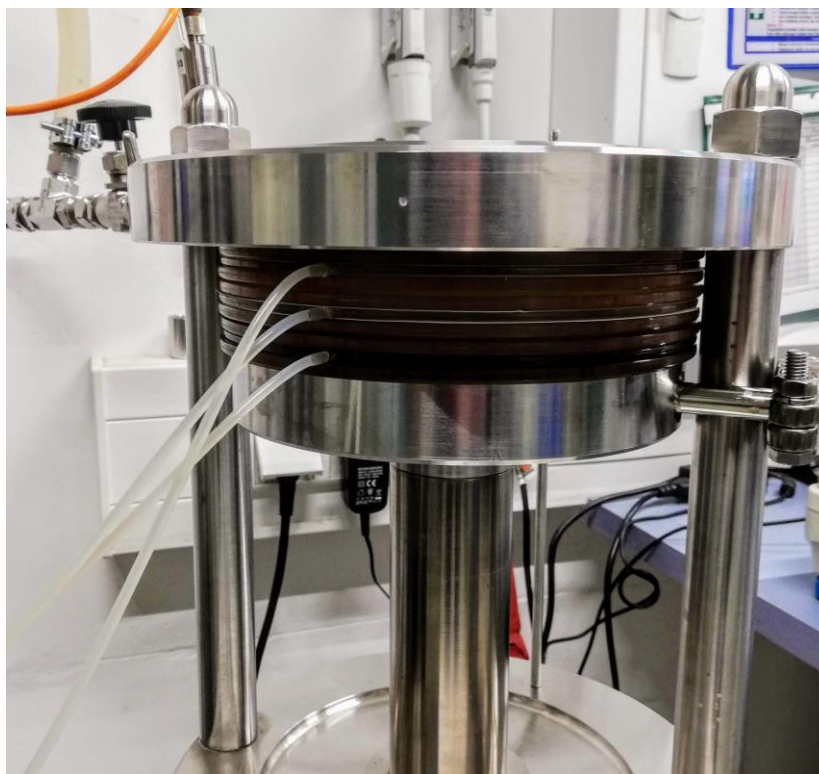


Figure 3.6: The Alfa Laval LabStak M20 membrane filtration assembly

Three types of commercial NF membranes were chosen to undergo parallel screening for optimal permeate flux and MCFA retention. The membranes chosen were the Tricep TS80, the NP030-P from Microdyn Nadir (USA) and the ETNA01PP from Alfa Laval (Denmark). Two sheets of each of the composite polymer membranes were cut to size and installed in the Labstak M20 unit, giving a total filtration surface area of 0.036 m^2 per membrane. The membranes were chosen to have an isoelectric point of around pH 4, which is lower than the pH of the feed, so that the MCFA rejection could be maximised by the negative surface charge. The membranes each have different functional groups on the active layer and were chosen to represent a range of MWCOs between 150 and 1000 Da. Full details of all membrane properties available from the manufacturers or the literature are presented in Table 3.1.

Table 3.1: NF Membrane Properties. Data are sourced from the manufacturer or literature, as noted. Discrepancies in parameter values generally relate to measurements being conducted under different conditions.

| <i>Manufacturer</i> | Microdyn Nadir | Microdyn Nadir | Alfa Laval |
|---|-----------------------------------|-----------------------|-------------------------------------|
| Membrane Type | Trisep TS80 (110) | NP030 P (111) | ETNA01PP (112) |
| Membrane Material | Thin-film semi-aromatic polyamide | Polyethersulfone | Composite fluoropolymer |
| Support Material | Non-woven polyester | Polypropylene | Polypropylene |
| MWCO (Da) | 150 (113) | 400 (114) | 1000 |
| Surface Area (m²) | 0.0174 | 0.0174 | 0.0174 |
| Pore Width (nm) | 0.36 (115) | 11.7 (116) | - |
| Zeta Potential [pH] (mV) | -19.9 [5.6] (117), -12 [>6] (115) | - | - |
| Isoelectric Point (pH) | 4 (118) | 3.4 (119) | - |
| Contact Angle (°) | 48.7, 43 (118) | 58,0 (116) | - |
| Membrane Thickness (μm) | 11 | - | - |
| Permeability (l h⁻¹m⁻² bar⁻¹) | 5.2 (118), 20 (113) | 1.7, 2.2 (114) | 15.5, 8.75 (120), 33 (121) 29 (122) |
| MgSO₄ retention (%) | 98.5 | 80-95 (116) | 26.3 |
| Na₂SO₄ retention (%) | 80-90 | 80-95 | 54.7, 27 (121) |
| NaCl retention (%) | 80-90 | | 9.1 (120), 17 (121) |
| Operating Pressure (bar) | 8 | < 40 | 1 - 10 |
| Temperature Range (°C) | < 45 | < 70 | 5 – 60 |
| pH range | 1 - 12 | 0 - 14 | 1 - 11 |

3.5.2 Methods

In both UF and NF experiments, the volume reduction (*VR*) is defined as in equation 3.1, where V_f is the original feed volume and V_p is the permeate volume.

$$VR = \frac{V_p}{V_f} \quad (3.1)$$

UF Concentration Experiments

Based on the critical flux determination, as well as published (123) and in-house experience, the process parameters listed in Table 3.2 were chosen for the

subsequent UF experiments. A temperature of 40°C was chosen as it is close to that in the fermentation process.

Table 3.2: UF process parameters

| Parameter | TMP | Feed Flowrate | CFV | Temperature |
|-----------|-----|---------------------|-------------------|-------------|
| Unit | bar | L min ⁻¹ | m s ⁻¹ | °C |
| Value | 3.0 | 20 | 1.7 | 40 |

Sequence One: Pre-experiment (Exp. 1.3)

To produce feed for the NF membrane screening experiments, 86.6 kg of thermally treated FB was filtered through the 15 kD UF membrane under the conditions detailed in Table 3.2.

Sequence Two: Cascade Experiments (Exp. 2.3/4/5/6)

The UF concentration experiments were performed with 25 kg of the fermentation broth for each path in the filtration cascade (Figure 3.2) under the conditions detailed in Table 3.2. The UF concentration experiments were terminated at a volume reduction of ~0.9 when the feed volume had reached the minimum recommended by the filtration unit manufacturer.

NF Membrane Screening (Exp. 1.4)

The screening was performed by recirculating 7 L of thermally treated 15 kD UF permeate from Exp. 1.3 for 2 h at 40°C (TMP = 8 bar, CFV = 1.1 m s⁻¹) until the flux was stable. In recirculation mode, the permeate flux through each membrane was measured under the same conditions at TMP values of 8, 10, 20, 30, 40 and 50 bar and samples were taken at each point for analysis. To investigate the relationship between feed flow rate and flux and to attempt to reduce fouling by promoting turbulent flow, the experiment was repeated at a TMP of 30 bar with flowrates of 10.0, 13.3, 16.7, 20.0 and 23.8 L min⁻¹.

NF Concentration Experiments (Exp. 2.7/8/9/10)

After selecting the Trisep TS80 as the optimal membrane, NF concentration experiments were performed with 10 kg of UF permeate from each of the four pretreatment paths. The process parameters were selected based on the results of the NF screening experiments and are listed in Table 3.3. The first NF concentration experiment (Exp. 2.7) was stopped after 360 min at a VR of 0.61, when the feed flux had reached <10% of the initial value. To understand more about the fouling mechanisms, the pure water flux (PWF) was measured after rinsing and cleaning and the retentate was reintroduced into the feed tank. The filtration was continued to overall VR of 0.65 when the flux had again reached a minimum. The subsequent filtrations (Exp. 2.8/9/10) were stopped after 360 min, once the VR had reached ~0.6.

Following the cleaning cycle after experiment Exp. 2.9, PWF and MgSO_4 retention data indicated that the membrane was ruptured. The membrane was replaced, cleaned, and conditioned before use in Exp. 2.10 and Exp. 3.1.

Table 3.3: NF Concentration Experiment Process Parameters

| Parameter | TMP | Feed Flowrate | CFV | Temperature |
|-----------|-----|---------------------|-------------------|--------------------|
| Unit | bar | L min^{-1} | m s^{-1} | $^{\circ}\text{C}$ |
| | 30 | 10 | 1.11 | 40 |

Diafiltration (DF) (Exp. 3.1)

In an attempt to increase the membrane flux and volume reduction, and to better understand the fouling mechanisms, an experiment was conducted in DF mode -essentially, feed dilution. Around 9 kg of thermally treated 15 kD UF permeate from Exp. 2.3 was concentrated over 210 min to a VR of ~0.5 under the same conditions as the NF concentration experiments. A volume of deionised water with a mass equal to that of the collected permeate was then added to the feed tank and the concentration repeated. This was repeated four times (DF volume ratio of 2) before the feed was concentrated to a VR of 0.68 over 360 min, a total process time of 1200 min. Samples were analysed from the permeate and retentate, as well as the precipitate from the retentate after storage at 4 $^{\circ}\text{C}$ for 3 days.

Pure Water Flux Measurements

PWF experiments were conducted to compare the ideal permeability of the membranes and quantify fouling by assessing their pre- and post-filtration performances. As deionised water contains no solutes or particles that can cause fouling, the pure water permeate flux (q_w) can be modelled by using a slightly modified version of Darcy's law (Equation 3.2) where ΔP is the transmembrane pressure (TMP), μ is the absolute viscosity, and R_m is the hydraulic resistance.

$$q_w = \frac{\Delta P}{\mu R_m} \quad (3.2)$$

The hydraulic resistance term (R_m) is a function of membrane properties and can be modelled by equation 3.3 where τ is the tortuosity of the pores, r their radius, Δz their length and ρ_{pore} their number density.

$$R_m = \frac{8\tau\Delta z}{\pi r^4 \rho_{pore}} \quad (3.3)$$

The pore radius term (r) in equation 3.3 is raised to the fourth power and has, therefore, the most influential factor in the hydraulic resistance. The PWF (q_w) was determined by weighing the permeate (m) for a duration of 60 sec (Δt) at intervals of 5 min until three successive stable measurements were obtained and calculated as per equation 3.4 where A is the surface area of the membrane.

$$q_w = \frac{m}{A\Delta t} \quad (3.4)$$

Since the PWF for a ceramic membrane is a function only of the TMP (ΔP), the hydraulic permeability (P_w) can be determined from the slope of the line obtained by measuring the permeate flow rate (q_w) over a range of pressures (Equation 3.5).

$$P_w = \frac{q_w}{\Delta P} \quad (3.5)$$

PWF measurements were taken before each experiment, after filtration and rinsing with water, and after each cleaning step. The PWF was measured with deionised water ($<10 \mu\text{S cm}^{-1}$) at 25 °C. For UF the CFV used was 1.7 m s⁻¹ and the TMP values were 1, 2, 3, and 4 bar. For NF, the CFV was 1.1 m s⁻¹ and the TMP values were 10, 20, 30 and 40 bar.

Fouling Analysis from PWF

A characterisation of flux losses during filtration was obtained from the PWF data by calculating the contributions caused by (a) irreversible fouling (b) reversible fouling and (c) concentration polarisation.

Flux loss resulting from irreversible mechanisms such as recalcitrant pore blockage, adsorption, and pore contraction (q_{irr}) was calculated as per equation 3.6. This flux loss is given by the difference between the original PWF (q_{PWF}) and post-cleaning PWF (q''_{PWF}), after the application of chemical cleaning agents.

$$q_{irr} = q_{PWF} - q''_{PWF} \quad (3.6)$$

Flux loss resulting from reversible fouling mechanisms such as gel/cake layer formation (q_{rev}) was calculated as per equation 3.7. This flux loss is given by the difference between post-cleaning PWF (q''_{PWF}) and post-rinsing PWF (q'_{PWF}) without chemical cleaning.

$$q_{rev} = q''_{PWF} - q'_{PWF} \quad (3.7)$$

The flux loss component attributable to the osmotic pressure caused by concentration polarisation (at a given VR) was calculated as per equation 3.8 from the difference between the filtration flux with the substrate and the PWF chemical cleaning.

$$q_{CP} = q - q''_{PWF} \quad (3.8)$$

Using the resistance-in-series model, the PWF data were then used to quantify the membrane resistances that can be attributed to each individual mechanism of fouling (89). This model assumes that the total resistance (R_t) can be considered a sum of each partial resistance (equation 3.9) which allows them to be more easily estimated from the flux reduction values above and the Darcy Equation (3.2).

$$R_t = R_m + R_{irr} + R_{rev} + R_{CP} \quad (3.9)$$

Critical Flux Determination

To determine the critical flux of the UF membranes with the substrate in this study, the process was run in total recirculation mode for 3 h with a TMP of 3 bar until the flux was constant. The TMP was reduced to 1 bar, and when stable, the permeate flux was measured gravimetrically as in the PWF determination. Flux measurements were also taken at a TMP of 2, 3, and 4 bar, and the critical flux was determined from the point on the graph of TMP vs. flux where it deviates from the linear relation.

Cleaning and Conditioning

After each experiment, the membrane was cleaned using a 1 % solution of the alkaline cleaning agent P3-Ultrasil-53 (Ecolab, Germany) followed by a citric acid solution of pH 2.2 (IWV Reagents, Germany; $\geq 99.5\%$). Cleaning was performed with 7.5 L of the solution for 40 min at 40 °C with a TMP of 4 bar and a CFV of 1.7 m s^{-1} . After cleaning, the membrane was flushed with deionised water until the conductivity was $<10 \text{ mS cm}^{-1}$ and the PWF was measured. Before use, the NF membranes were conditioned by compaction at a TMP of 10 bar for 2 h to avoid pressure effects in subsequent experiments.

Kjhkj

MgSO₄ Retention

To monitor changes in the permeability of solutes through the NF membranes, the MgSO₄ rejection was measured before and after each experiment. A feed of $\sim 2000 \text{ ppm}$ MgSO₄ (Roth, Germany; $\geq 99\%$) in deionised water was recirculated for 15 min over the membrane with a TMP of 9 bar, CFV of 1.1 m s^{-1} and temperature of 25°C. The electrical conductivity of the feed (σ_f) and the permeate (σ_p) were measured as in and the MgSO₄ rejection percentage (RC_{Mg}) was calculated (Equation 3.10).

$$RC_{Mg} = \frac{\sigma_f - \sigma_p}{\sigma_f} * 100\% \quad (3.10)$$

Acidification Trials

To better understand the composition of the NF retentate and identify potential membrane foulants, titrations with concentrated sulfuric acid were performed (H_2SO_4 , 90%). A 100 mL sample of the retentate from Exp. 2.7 was taken and its pH measured with the stepwise addition (100 μL) of the acid. Phase separation and the formation of precipitates were observed.

3.6 Chemical and Physical Analysis

3.6.1 MCFA Quantification by GC

The MCFA concentrations were measured as methyl ester derivatives of the acids with an Agilent 7980 A GC (USA) using a PerkinElmer TurboMatrix HS 110 automated headspace sampler (USA). Esterification was performed directly in the 20 mL glass sample vials by adding 0.5 mL of methanol and 2.5 mL of aqueous sulphuric acid (20% v/v) to 0.3 mL of the sample along with 1.7 mL of deionised water and 1 mL of aqueous 2-methylbutanoic acid (184 mg L^{-1}) as an internal standard. The vials were sealed with crimp caps and stored at 4 °C before being analysed in triplicate under the conditions listed in (Table 3.4). From the GC analysis, the MCFA retention coefficient (RC) was calculated as in equation 3.11, where C_p and C_f are the MCFA concentrations in the permeate and feed, respectively.

$$RC = 1 - \frac{C_p}{C_f} \quad (3.11)$$

Table 3.4: GC analysis parameters

| Parameter | Value |
|----------------------------|--|
| Injector | Split-Splitless, 220 °C |
| Split ratio | 10:1 |
| Carrier gas | Nitrogen |
| Column | DB-FFAP (60 m x 0.25 mm x 0.5 μm) |
| Detector | Flame ionisation detector |
| Temperature program | <ul style="list-style-type: none"> Initial temperature of 40 °C held for 20 min Heating gradient of 10 °C min⁻¹ for 16 min Temperature held at 200 °C for 10 min |
| Total run time | <ul style="list-style-type: none"> 46 min |

3.6.2 Chemical Oxygen Demand (COD)

COD measurements were performed as per ISO 15705 (124). A 50 μL aliquot of each sample was added to pre-prepared LCK 014 COD Cuvettes from the manufacturer Hach (Germany), shaken and heated at 148 $^{\circ}\text{C}$ for 2 h. After cooling, the absorbance at 605 nm was measured with a DR 3900 UV-Vis Spectrometer (Hach, Germany) and the COD was calculated by the instrument.

3.6.3 Density

Density was determined by weighing 100 mL of sample on an analytical balance (sensitivity 0.1 mg) in a type B volumetric flask.

3.6.4 Dry Residue and Water Content

Determination of dry residue and water content was performed in triplicate as per the European standard DIN EN 12880:2000 (125). Between 10 and 60 g of the sample was weighed into a ceramic crucible and placed in a drying cabinet at 105 $^{\circ}\text{C}$ for 24 h. After cooling in a desiccator, the crucible was weighed again, then the dry residue (w_{dr}) and water content (w_w) were calculated as a weight percentage according to equations 3.12 and 3.13

$$w_{dr} = \frac{(m_c - m_a)}{(m_b - m_a)} \times 100 \quad (3.12)$$

$$w_w = \frac{(m_b - m_c)}{(m_b - m_a)} \times 100 \quad (3.13)$$

where m_a is the mass of the crucible, m_b the mass of the crucible and sample and m_c the mass of the crucible and sample after drying.

4. Results and Discussion

4.1 Basket Press Filtration

The basket press effectively removed coarse solids from the FB and reduced the dry residue on average from 6.8 to 2.2% w/w in the liquid phase. Over both experimental phases, the average liquid recovery from the FB slurry was 81.9% and the average dry residue of the filter cake was 18.3%. The liquid retained in the filter cake amounts to a considerable loss of MCFAs and this process step could certainly be improved by process or equipment optimisation. For example, flushing of the filter cake with gas or rinsing with process water (NF permeate) could improve MCFA recovery, although the latter would increase membrane filtration process volumes and decrease product concentration.

The basket press used in this study did not allow for cake rinsing, and previous studies with a benchtop decanter-centrifuge proved unsatisfactory due to the very large, low-density particles in the FB. Alternative equipment such as a plate-and-frame filter or a belt filter would likely be more suitable since both would allow for cake washing and the belt filter for continuous filtration (126, 127). Examples of the feed, filter cake, and filtrate are depicted in Figure 4.1, a partial mass balance of each basket press filtration is listed in Table 4.1, and a full analysis is detailed in appendix 7.1.



Figure 4.1: The feed, filtrate, and filter cake of the basket press filtration (from left to right)

Table 4.1 A partial mass balance of the basket press filtration

| Experiment | Feed Mass | Feed Solids | Filtrate Mass | Filtrate Dry Residue | Liquid Recovery |
|--------------------|-----------|-------------|---------------|----------------------|-----------------|
| | <i>kg</i> | % w/w | <i>kg</i> | % w/w | % |
| Phase 1 (Exp. 1.1) | 136.4 | 6.8 | 107.9 | 2.5 | 83 |
| Phase 2 (Exp. 2.1) | 133.3 | 6.5 | 103.9 | 2.0 | 81 |

4.2 Thermal Treatment

In both cases (Exp. 1.1 & 2.1), thermal treatment of the FB caused the colour to darken, though no substantial flocculation or precipitation was observed (Figure 4.2). Thermal treatment caused the COD to decrease from 60.2 to 53.7 g L⁻¹ due to heat-induced oxidation. A small decrease in the dry residue was measured in each case (0.06 & 0.20 % w/w) but this was not substantial. No considerable change in density, conductivity or FA concentration was observed post thermal treatment (Table 7.1, Table 7.2). The influence of thermal treatment on membrane flux is discussed in the following sections.

**Figure 4.2:** The filtered FB before (left) and after (right) thermal treatment

4.3 Membrane Filtration - Sequence One

UF and NF membrane and parameter screening

4.3.1 Ultrafiltration (Exp. 1.3)

Using the thermally treated FB from Exp. 1.2, the critical flux was determined to lie between 2 and 3 bar (Figure 4.3). The deviation from the linear increase of flux with pressure after 2 bar indicates the transition to the limited flux phase. As the cause of flux limitation in this case may be attributed to concentration polarisation and gel/cake layer formation (96), the result could be generalized and assumed to approximate for the 150 kD membrane and the non-thermally-treated FB.

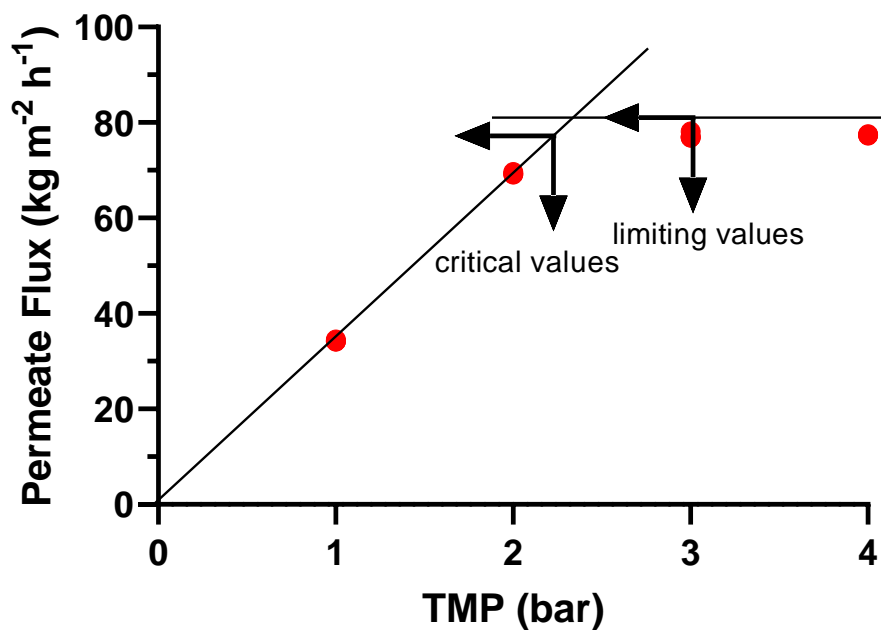


Figure 4.3: Experimental determination of the critical flux for the thermally-treated FB by UF on the 15 kDa membrane

As a proof of concept, the filtration of the complete first batch of FB indicated that the process could be sustainable on a large scale. In the first 100 min (VR = 0.2), the flux decreased only 10% from the initial value of 60 kg m⁻² h⁻¹ to 54 kg m⁻² h⁻¹, and this flux was maintained until the feed was no longer refilled (500 min, VR = 0.77). Although the flux decreased with time as the feed became more concentrated,

periodic refilling of the feed tank resulted in increased flowrates which suggests that flux decline is related to reversible fouling and increases in concentration and viscosity (Figure 4.4). The filtration was halted after 630 min, at a VR of 0.87, when the feed volume reached the minimum recommended by the manufacturer.

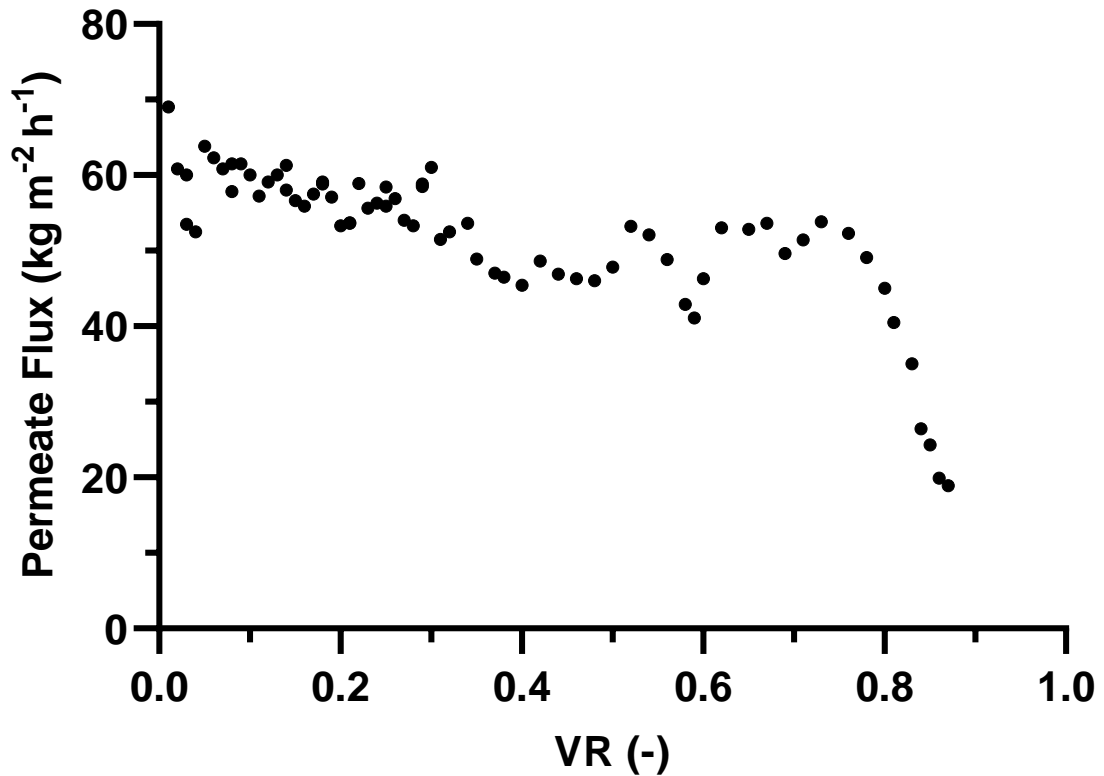


Figure 4.4: Permeate flux vs. volume reduction (VR) for UF in concentration mode of 86.6 kg of thermally treated FB on the 15 kD membrane (630 min, 3 bar, 40°C, 1.7 m s⁻¹)

No change in FA concentration was measured as a result of the UF, in each case, the rejection coefficient was less than 0.1 (Table 7.3). The UF reduced the dry residue from 2.5% to only 2.3%, which indicates that the largest proportion of residue is from dissolved salts and small molecules (Table 7.1). Photos of UF permeate and retentate are presented in Figure 4.5.



Figure 4.5: The typical UF permeate (left) and retentate (right)

4.3.2 Nanofiltration Membrane Screening (Exp. 1.4)

Permeate Flux

The permeate flux of each NF membrane as a function of TMP was linearly proportional ($R^2 > 0.96$) over the pressure range tested (8-50 bar) (Figure 4.6). This indicates that, unlike in the UF, gel/cake layer formation is not a dominant resistance factor. As expected, the average permeability of each membrane correlated to its MWCO (Table 4.2). However, while the permeability of the ETNA01 decreased with TMP and that of the NP030 was roughly stable, the permeability of the TS80 increased at higher pressures and became higher than that of NP030 above 30 bar. Considering that 40 bar is the typical limit for many NF membranes, and as a compromise between energy cost and flux, a TMP of 30 bar was used for all subsequent NF experiments.

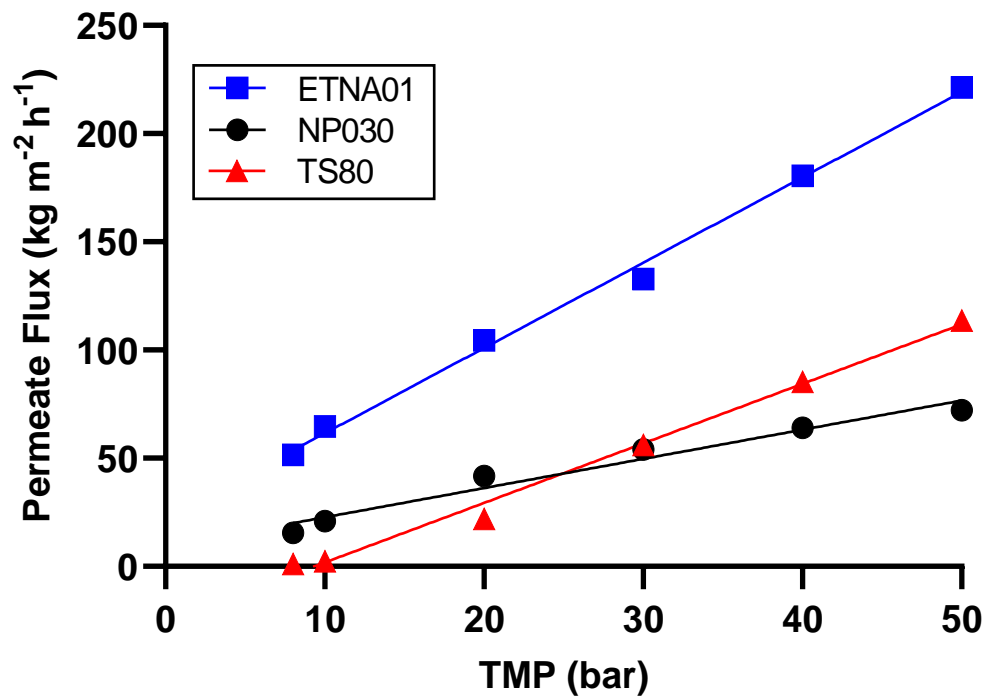


Figure 4.6: Permeate flux vs. transmembrane pressure (TMP) for the NF membranes ETNA01, NP030, and TS80 in total recirculation mode (40°C, CFV = 1.11 m s⁻¹)

Table 4.2: Permeability of the NF membranes as a function of TMP

| Permeability (kg h ⁻¹ m ⁻² bar ⁻¹) | | | | | | | |
|--|------|------|------|------|------|------|----------------|
| <i>TMP (bar)</i> | 8 | 10 | 20 | 30 | 40 | 50 | <i>Average</i> |
| ETNA01 | 6.43 | 6.47 | 5.22 | 4.43 | 4.51 | 4.43 | 5.25 |
| NP030 | 1.93 | 2.09 | 2.08 | 1.80 | 1.60 | 1.44 | 1.83 |
| TS80 | 0.16 | 0.24 | 1.10 | 1.87 | 2.13 | 2.27 | 1.29 |

Crossflow Velocity (CFV)

Although CFV is generally correlated to turbulence, decreased fouling and increased flux due to reduced concentration polarisation (128), the CFV had no appreciable influence on permeate flux for all the membranes tested (Figure 4.7). The likely reason for this is that, due to structure of the filtration plate (129), the feed flow across the membrane surface was already turbulent at the lowest CFV, thus there was no additional foulant removal at higher velocities (128). As it was the most economical, the lowest CFV (1.11 m s^{-1}) was used for all subsequent NF experiments.

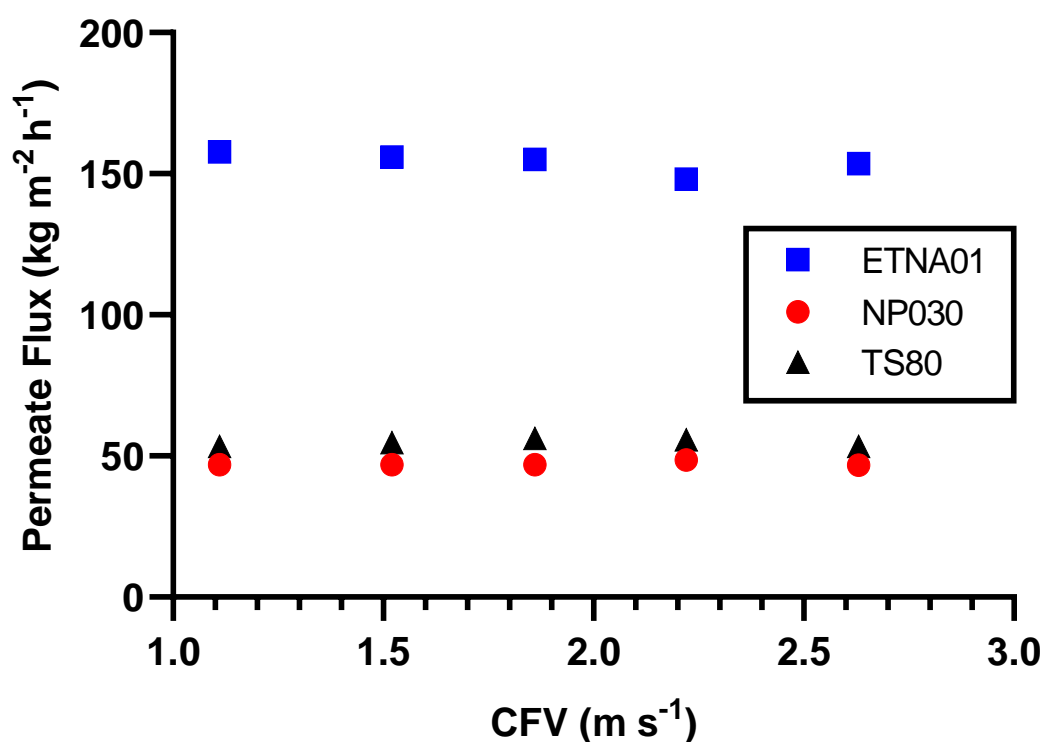


Figure 4.7: Permeate flux vs. crossflow velocity (CFV) for the NF membranes ETNA01, NP030, and TS80 in total recirculation mode (40°C , $\text{TMP} = 30 \text{ bar}$).

Fatty Acid Retention

The retention of C2-C8 FAs was, as expected, directly proportional to the tightness of the membrane: ETNA01 (MWCO 1000 Da), 14–33%; NP030 (MWCO 400 Da), 40–65%; TS80 (MWCO 150 Da), 92–98% (Table 7.4). This was also seen in the average MgSO_4 retentions, which were 25, 40 and 95% for the ETNA01, NP030, and TS80 membranes respectively.

The retention of all FAs was shown to be proportional to the TMP for all membranes, a result which is in agreement with similar NF studies with lactic acid (128, 130). This effect was greatest for the NP030 (avg. $+0.57\% \text{ bar}^{-1}$) compared to the TS80 (avg. $+0.18\% \text{ bar}^{-1}$) and ETNA01 (avg. $+0.13\% \text{ bar}^{-1}$) membranes. This effect is attributed to the increased permeate flux, which leads to the formation of a gel/cake layer that adds an additional barrier and thus greater retention (131).

Selectivity between the C2-C8 FAs was observed for all membranes (Table 7.4). This was especially so for the ETNA01, whose average rejection of C6 and C8 was reduced by 25% and 50% respectively, compared to C2 and C4 acids. This is the opposite trend to that expected from size exclusion and could be explained by charge effects, whereby the larger, more hydrophobic FAs have a higher affinity to the membrane than the smaller, more polar C2 and C4 acids. For the tighter membranes, the reverse of this was observed, and rejection was shown to be a function of MW.

This was especially so for the NP030, by which the absolute rejection rose an average of 5% with each successive increase in FA chain length. The TS80 membrane, which had a very high rejection (92–98%) of all FAs, was only slightly more permeable ($+1.5\%$) for the smallest acid, C2.

Because of its high FA retention, and despite having only around one-third of the flux of ETNA01, the TS80 was selected as the optimal membrane for the second phase of this study.

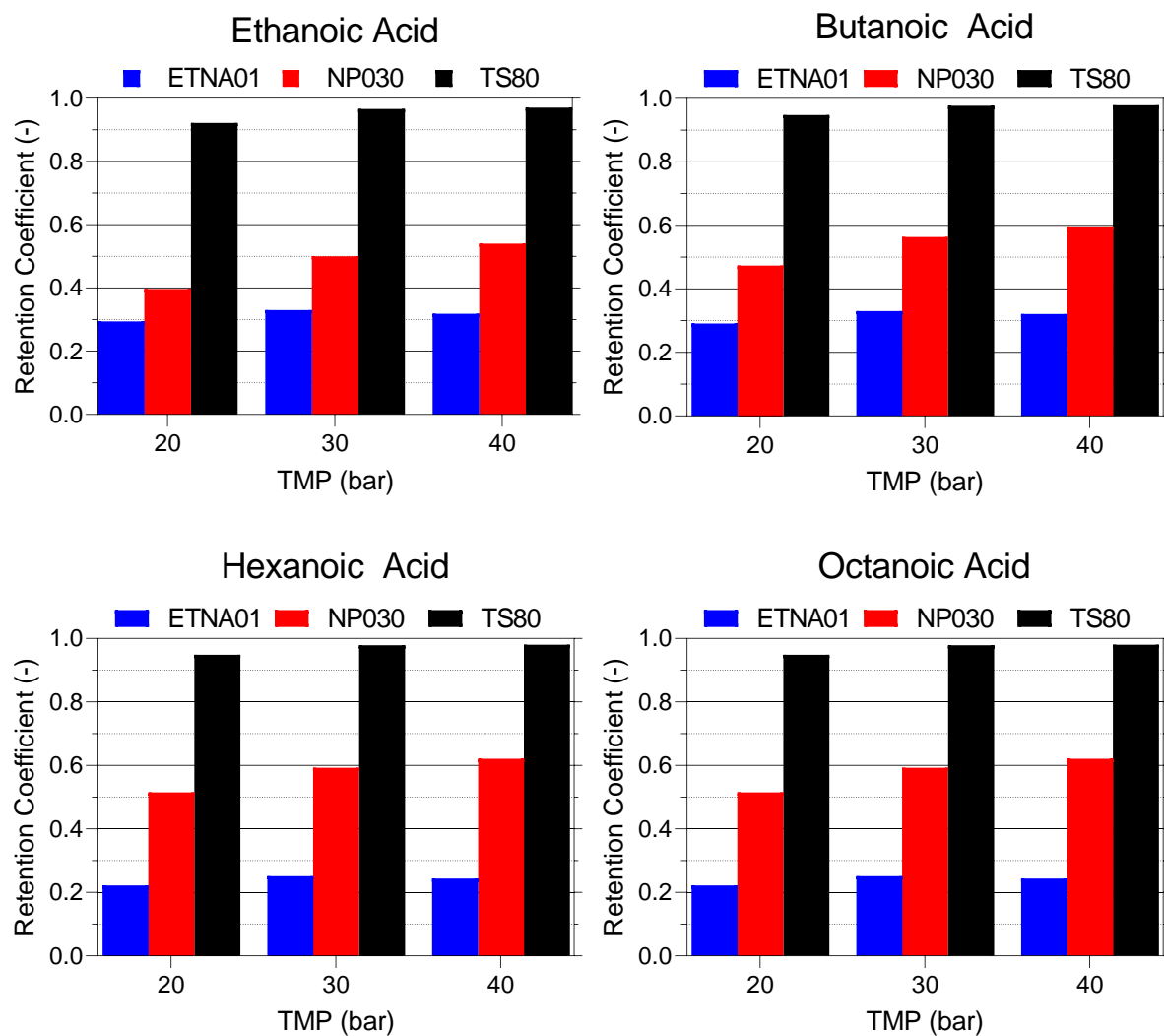


Figure 4.8: Rejection coefficients for the C2-C8 FAs as a function of TMP for the NF membranes ETNA01, NP030, and TS80

4.4 Membrane Filtration - Sequence Two

Pretreatment Screening and Diafiltration

4.4.1 Ultrafiltration (Exp. 2.3/4/5/6)

Permeate Flux

In each of the UF concentration experiments, a VR of ~ 0.9 was achieved within 160 to 195 minutes. The flux remained relatively stable at $\sim 55 \text{ kg m}^{-2} \text{ h}^{-1}$ until a VR of 0.5, after which it began to decline, finally reaching $\sim 20 \text{ kg m}^{-2} \text{ h}^{-1}$. This is comparable to other studies with similar filtration systems (30, 132). Of the four UF feeds, the one outlier is the untreated FB 15 kD (Exp. 2.4) where the flux increased from an initial value of 40.3 up to a maximum of 55.1 $\text{kg m}^{-2} \text{ h}^{-1}$ (VR = 0.53), before declining uniformly with the others. This result is anomalous since although there was a small initial flux increase ($\sim 5 \text{ kg m}^{-2} \text{ h}^{-1}$) for the thermally treated FB on both the 15 and 150 kD membranes (Exp. 2.3 & 2.5), the initial flux of the untreated FB on the 150 kD membrane did not increase, remaining constant until a VR of 0.5. Such flux increases have been observed in other studies, though the cause remains unclear (133). The cause of the larger flux increase in Exp. 2.4 is possibly the result of process instability, whereby the TMP fluctuated and the temperature was $<40^\circ\text{C}$ at the beginning of the experiment.

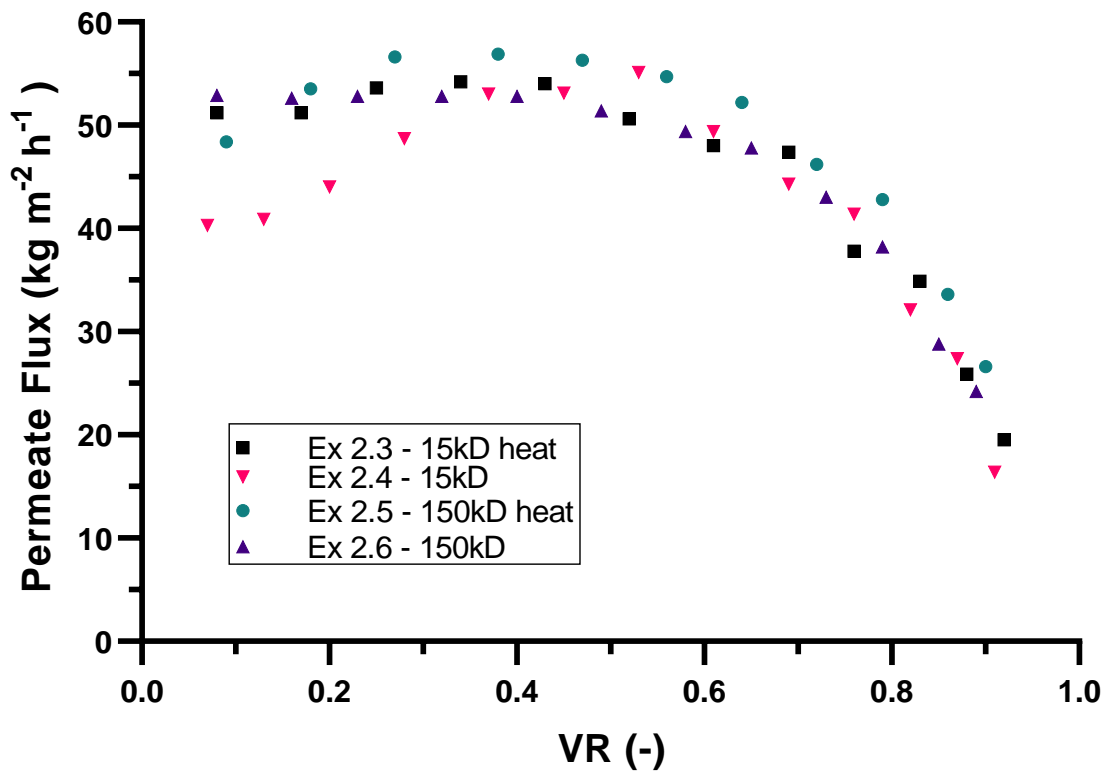


Figure 4.9: Permeate flux vs. volume reduction (VR) for the crossflow UF of pressed maize silage FB. (40°C, TMP = 3 bar, CFV = 1.66 m s⁻¹)

The data show that neither thermal treatment nor pore size had a substantial effect on UF flux. This is contrary to the published experience from the UF of dairy products, where thermal treatment resulted in enhanced permeate flux (107). While membrane permeability is typically proportional to average pore size, with complex mixtures such as FB it is not possible to generalise or predict the effect of pore size on permeate flux. Depending on the size of the particles in the feed with respect to the pores, flux decline can sometimes increase for larger pored membranes because the foulants can enter the pore entrances and cause internal fouling (90, 132).

In this study, however, the flux decline with both the 15 and 150 kD membranes was uniform, suggesting that the pore size was not a limiting factor for permeate flux. Thus, the dominant resistance was likely due to the development of a cake/gel layer on the membrane surface rather than from transport through the membrane itself. As the constitution of the cake layer depends much more on the feed than it does on the nature of the membrane, it follows that the permeate flux was very similar in each of the UF experiments.

Fatty Acid Retention

In each UF experiment, the retention coefficient of all measured FAs was very low (≤ 0.05) (Table 4.3). Such small retentions of low-MW FAs were expected for membranes with much larger relative pore sizes. As the UF permeate can likely be recycled back into the fermentation, the rejection of FAs in this stage cannot be considered a loss in the overall process.

Table 4.3: Average FA concentration (C2-C8) and retention coefficient for the UF of maize silage FB at a volume reduction of ~ 0.9

| Fatty Acid | C2 | C4 | C6 | C8 |
|---|-------------|-------------|-------------|-------------|
| Permeate Concentration (g L ⁻¹) | 8.91 | 2.73 | 2.21 | 0.31 |
| <i>Standard deviation</i> | <i>0.14</i> | <i>0.03</i> | <i>0.03</i> | <i>0.01</i> |
| Retentate Concentration (g L ⁻¹) | 9.34 | 2.96 | 2.32 | 0.34 |
| <i>Standard deviation</i> | <i>0.32</i> | <i>0.08</i> | <i>0.05</i> | <i>0.01</i> |
| Retention Coefficient | 0.02 | 0.05 | 0.03 | 0.04 |

Other Properties

The separation resulted, on average, in a slight decrease to the density ($- 10 \text{ g L}^{-1}$) and dry residue ($- 0.1\% \text{ w/w}$) of the permeate with were no apparent differences between the four experiments. The average COD of the permeate was 43 g L^{-1} , that of the retentate 118 g L^{-1} . The COD of the permeates from the 15 kDa membrane were slightly lower ($\sim 3 \text{ g L}^{-1}$) than those from the 150 kDa membrane because more organic macromolecules were separated. The thermal treatment caused a small decrease in COD of around 1.5 g L^{-1} in each case due to oxidation caused by heat.

4.4.2 Nanofiltration (Exp. 2.7/8/9/10)

Permeate Flux

In each of the NF concentration experiments, a VR of between 0.56 and 0.65 was achieved, and the highest initial fluxes were seen with the UF permeate from the 15 kD membrane (Figure 4.10). Of the two, the heated 15 kD feed had the best performance, with an initial flux of $77 \text{ kg m}^{-2} \text{ h}^{-1}$ compared to $67 \text{ kg m}^{-2} \text{ h}^{-1}$ for the unheated 15 kD feed. It was expected that the combination of thermal treatment and tight UF pore size would reduce the concentration of NF foulants the most, and thus Exp. 2.7 would have the highest permeate flux. While the flux was somewhat higher, the difference could relate to the condition of the membrane, as this was the first experiment conducted on a virgin filter.

While the heated 15 kD feed retained the highest flux until near the end of the concentration, the unheated 15 kD feed experienced more rapid flux decline, and after a VR of 0.35 had the lowest flux of all four feeds. Between the heated and unheated feeds from the 150 kD membrane, there was almost no difference in flux across the entire filtration. This could be because most of the organic macromolecules are removed by each of the different UF filtrations, therefore they do not cause fouling in NF and their denaturation is irrelevant. Unlike in UF where a relatively stable flux persisted until $\text{VR} > 0.6$, flux decline in the NF experiments was direct and linear ($R^2 > 0.99$). Despite the rapid decline, the permeate flux in this study compares favourably to that reported for the filtration with TS80 of model FB solution ($20 \text{ kg m}^{-2} \text{ h}^{-1}$) (134).

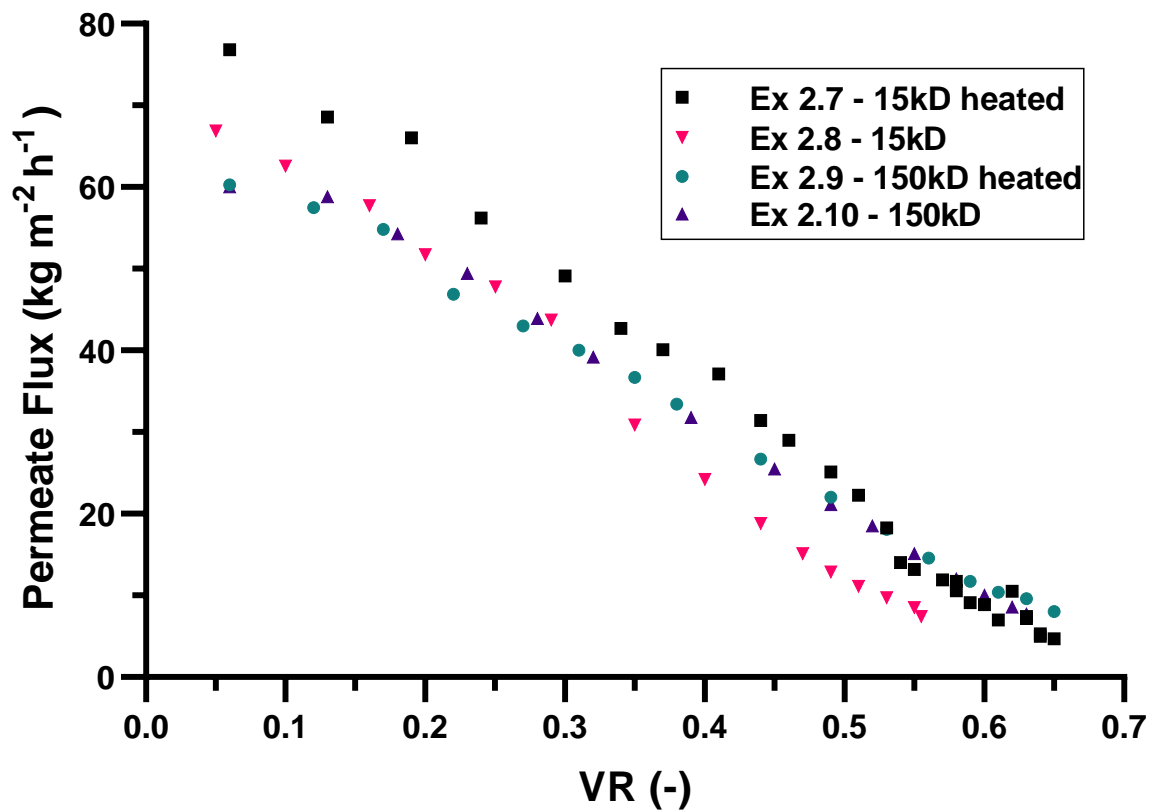


Figure 4.10: Permeate flux vs. volume reduction (VR) for the crossflow NF of UF permeate from pressed maize silage FB. (TS80 membrane, 40°C, TMP = 30 bar, CFV = 1.11 m s⁻¹).

Fatty Acid Retention

In each NF experiment, the average MCFA retention was 5-10% less than that measured in the membrane screening phase, indicating that the rejection of the acids is dependent on the concentration factor of the feed (Table 4.4).

Table 4.4: Rejection coefficients with respect to C2-C8 FAs for the NF membrane TS80 in the concentration experiments (Exp. 2.6-2.10 & 3.1)

| Fatty Acid Retention Coefficient (-) | | | | |
|--------------------------------------|-------|-------|-------|-------|
| Experiment | C2 | C4 | C6 | C8 |
| 2.7: 15 kD heated | 0.852 | 0.925 | 0.921 | 0.896 |
| 2.8: 15 kD | 0.893 | 0.938 | 0.932 | 0.909 |
| 2.9: 150 kD heated | 0.865 | 0.938 | 0.932 | 0.909 |
| 2.10: 150 kD | 0.853 | 0.922 | 0.920 | 0.898 |

The various pretreatments of the feed solution had, however, no significant effect on MCFA retention, as demonstrated by the small standard deviations from the average (Table 4.5). The retention of FAs here was higher than those reported a study with the TS80 membrane using model solutions of similar pH. In this study, the retention of acetic acid (0.46), and the larger, divalent succinic acid (0.26) were much lower, possibly due to the absence of membrane fouling, which can reduce the effective pore size (134).

Table 4.5: Average FA concentration (C2-C8) and retention coefficient for the NF of UF permeate from maize silage FB

| | Fatty Acid Concentration (g L⁻¹) | | | |
|------------------------------|--|-------------|-------------|-------------|
| | C2 | C4 | C6 | C8 |
| Permeate | 1.20 | 0.20 | 0.17 | 0.03 |
| <i>Standard deviation</i> | <i>0.14</i> | <i>0.02</i> | <i>0.01</i> | <i>0.00</i> |
| Retentate | 21.90 | 6.78 | 5.39 | 0.75 |
| <i>Standard deviation</i> | <i>1.78</i> | <i>0.62</i> | <i>0.45</i> | <i>0.05</i> |
| Retention Coefficient | 0.87 | 0.93 | 0.92 | 0.90 |

Other Properties

The separation resulted, on average, in the retentate having a small pH decrease (<1) and tenfold higher conductivity compared to the permeate. The COD of the permeate was reduced to 6.8 g L⁻¹, compared to 108 g L⁻¹ in the retentate and 40 g L⁻¹ in the feed (Exp. 2.7). This is expected, as the majority of acids, organic molecules, and divalent salts are retained by the membrane.

The NF permeate was colourless and had a strong ammonia-like odour, whereas the retentate had clear, dark brown colour and an odour reminiscent of goats, characteristic of C6 and C8 FAs. Photographs of a typical NF feed, retentate and permeate are depicted in (Figure 4.11).



Figure 4.11: Photographs of the typical NF retentate and permeate from the concentration of UF permeate from maize silage FB with a TS80 membrane (left to right)

4.4.3 Diafiltration (DF) (Exp. 3.1)

Permeate Flux

The effect of DF on permeate flux was generally negligible, though, toward the end of each concentration ($VR > 0.5$), a small flux increase ($\sim 4 \text{ kg h}^{-1} \text{ m}^{-2}$) was observed after the third and fourth dilutions (Figure 4.12). This minor benefit comes, however, at a substantial time cost: the DF took 1200 min to reach a VR of ~ 0.65 , compared to 360 min for the standard NF concentrations.

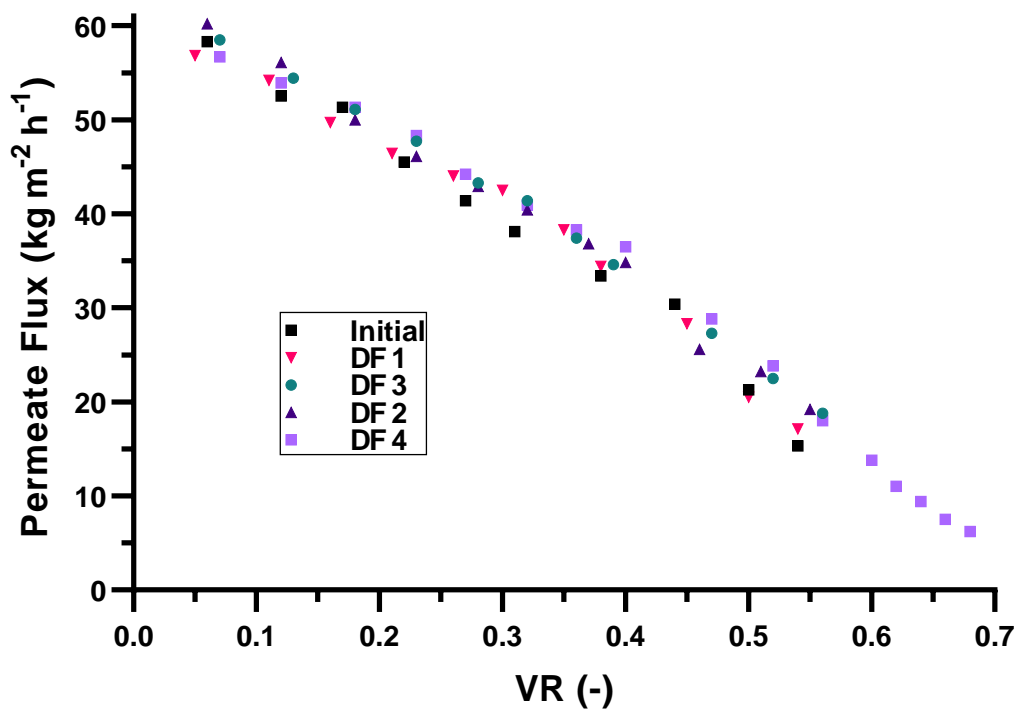


Figure 4.12: Permeate flux vs. volume reduction (VR) for the DF during NF of UF (15 kD) permeate of thermally-treated FB.

Fatty Acid Retention

The dilution by diafiltration caused a substantial decrease (~13%) in the effective retention coefficient for each of the C2-C8 FAs (Table 4.6). The retention of ethanoic acid was most markedly reduced (32.8%), likely a result of its relatively higher polarity. The reduction in the retention of the FAs is unsurprising, as the diafiltration factor was 2, which amounts to a total permeate volume of ~24 kg compared to ~6 kg for the standard NF. Given the substantial additional costs in terms of yield, cost and time there appears to be no benefit in using DF for this application.

Table 4.6: FA concentration and retention coefficient for the DF during the NF of UF permeate from maize silage FB. The NF average is calculated from the retentions in Exp 2.7-2.10.

| Fatty Acid | C2 | C4 | C6 | C8 |
|---|-----------|-----------|-----------|-----------|
| Permeate Concentration (g L ⁻¹) | 3.72 | 0.48 | 0.45 | 0.06 |
| Retentate Concentration (g L ⁻¹) | 22.28 | 6.08 | 5.83 | 0.67 |
| Retention Coefficient | 0.58 | 0.82 | 0.79 | 0.79 |
| <i>Reduction from NF average (%)</i> | 32.8 | 11.2 | 14.2 | 11.9 |

4.4.4 Acidification Trials (Exp. 3.2)

In an attempt to understand more about the composition of the NF retentate, titration with H₂SO₄ (98%) was performed. This showed a buffer zone around the pK_a of the FAs (~4.8) and separate precipitations at pH 3.9 and 2.9 (Figure 4.13). The precipitate at 3.9 was white and cloudy, whereas that at 2.9 was a fine brown particulate. A clear, oily residue and an insoluble brown deposit were present on the glassware and are suspected to comprise of C6/C8 FAs and humic acids, respectively. Further isolation steps and analysis would be necessary to confirm this. While direct separation of the FAs by acidification appears possible, the large quantity of acid required would make the process uneconomical. Alternative techniques such as electrolysis or extraction could prove more appropriate (49).

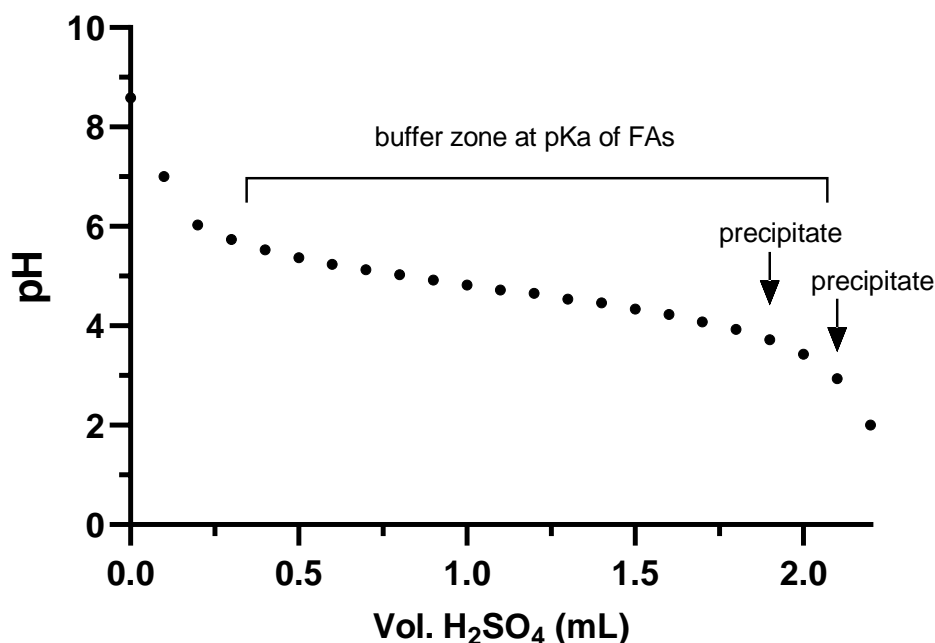


Figure 4.13: Titration curve for the NF retentate with the addition of H₂SO₄ (98%)

4.5 Fouling Analysis

4.5.1 Ultrafiltration

For both the 15 and 150 kD membranes, each of the first two filtration experiments caused a considerable (~40%) decline in pure water permeability which could not be recovered by chemical cleaning (Table 4.7, Table 4.8). The graphs of PWF show a consistent, but decreasing drop with each experiment compared to the virgin membrane (Figure 4.14, Figure 4.15).

It appears that the virgin membranes suffer substantial, irreversible fouling during their initial use when the larger pores become permanently blocked, resulting in an average recovery of only ~60%. After the third and fourth filtrations on the 15 kD membrane, recovery increased to 80, then 90%, indicating a stabilisation in flux decline as the most easily blocked pores were already saturated by foulants.

After Exp. 2.4 the PWF was also measured after rinsing with water to quantify the flux decline due to reversible fouling. For the 150 kD membrane, comparison of

the PWF after rinsing to that after cleaning shows roughly equal contributions from reversible and irreversible fouling. For the 15 kD membrane, the reversible fouling was more than four times greater than the irreversible fouling and supports the notion that larger pores are more susceptible to pore blocking (90). Given the significant variations in the PWF over time, it is difficult to infer any influences from the FB pretreatment on fouling. To achieve more reliable results and quantify relative fouling effects, it would be necessary to operate the membranes for many more cycles, until such time that the PWF is stable. Further investigations would also be required to determine the optimal cleaning regime, which for bio-foulants could require enzymes or more aggressive chemicals such as chlorine (108).

Table 4.7: The pure water permeability, flux recovery, fouling contributions and MgSO₄ retention for the 15 kD ZrO₂ UF membrane over the four experimental cycles. Recovery is calculated as a percentage of the original permeability compared to that post-experiment: after rinsing with water (+rinse), and chemical cleaning (+clean) (TMP 10-40 bar, 40°C, CFV = 1.67 m s⁻¹).

| | Pure Water Permeability (kg h ⁻¹ m ⁻² bar ⁻¹) | | | | | % Decline due to Fouling | |
|-------|---|---------|----------|---------|----------|--------------------------|------------|
| | Original | + Rinse | Recovery | + Clean | Recovery | Irreversible | Reversible |
| Exp. | | | % | | % | % | % |
| 1.3 a | 162.43 | - | - | 94.64 | 58.27 | - | - |
| 1.3 b | 94.64 | - | - | 55.18 | 58.31 | - | - |
| 2.3 | 55.18 | - | - | 45.00 | 81.55 | - | - |
| 2.4 | 45.00 | 23.75 | 52.78 | 41.18 | 91.51 | 8.49 | 38.7 |

Table 4.8: The pure water permeability, flux recovery, fouling contributions and MgSO₄ retention for the 150 kD ZrO₂ ultrafiltration (UF) membrane over the two experimental cycles (TMP 10-40, 40°C, CFV = 1.67 m s⁻¹)

| | Pure Water Permeability (kg h ⁻¹ m ⁻² bar ⁻¹) | | | | | % Decline due to Fouling | |
|------|---|---------|----------|---------|----------|--------------------------|------------|
| | Original | + Rinse | Recovery | + Clean | Recovery | Irreversible | Reversible |
| Exp. | | | % | | % | % | % |
| 2.5 | 567.10 | 121.94 | 21.50 | 310.67 | 54.78 | 45.22 | 33.3 |
| 2.6 | 310.67 | 76.18 | 24.52 | 192.18 | 61.86 | 38.14 | 37.3 |

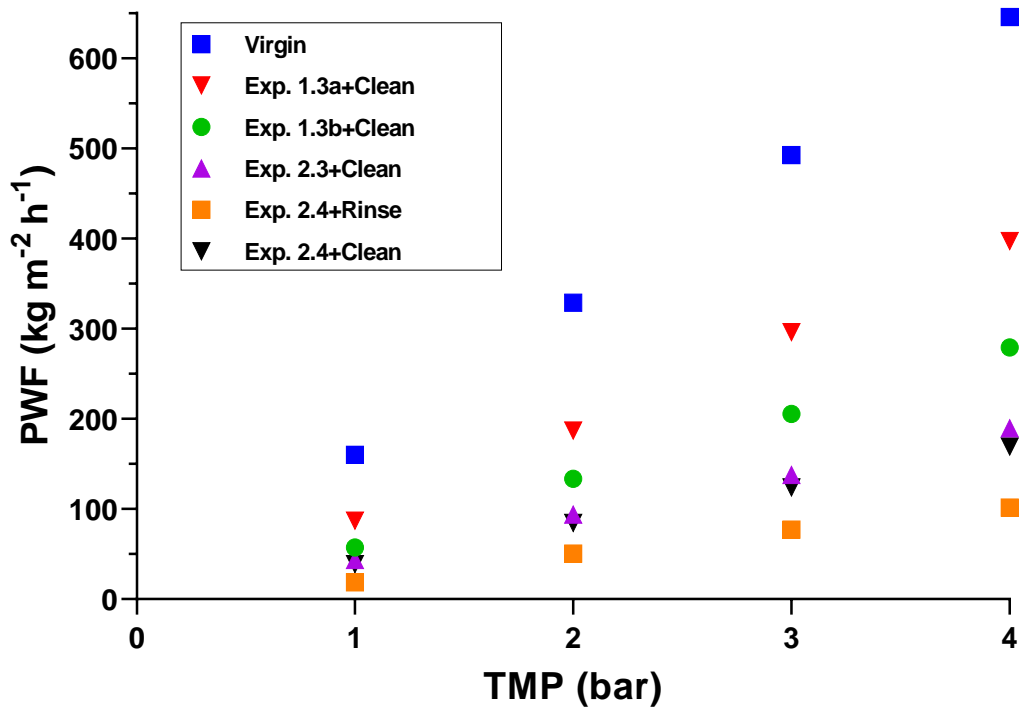


Figure 4.14: PWF vs. TMP of the 15 kD ZrO₂ membrane. The PWF was measured with the unused, cleaned membrane ("virgin"), after filtration and rinsing with water ("+rinse") and after the cleaning cycle ("+clean").

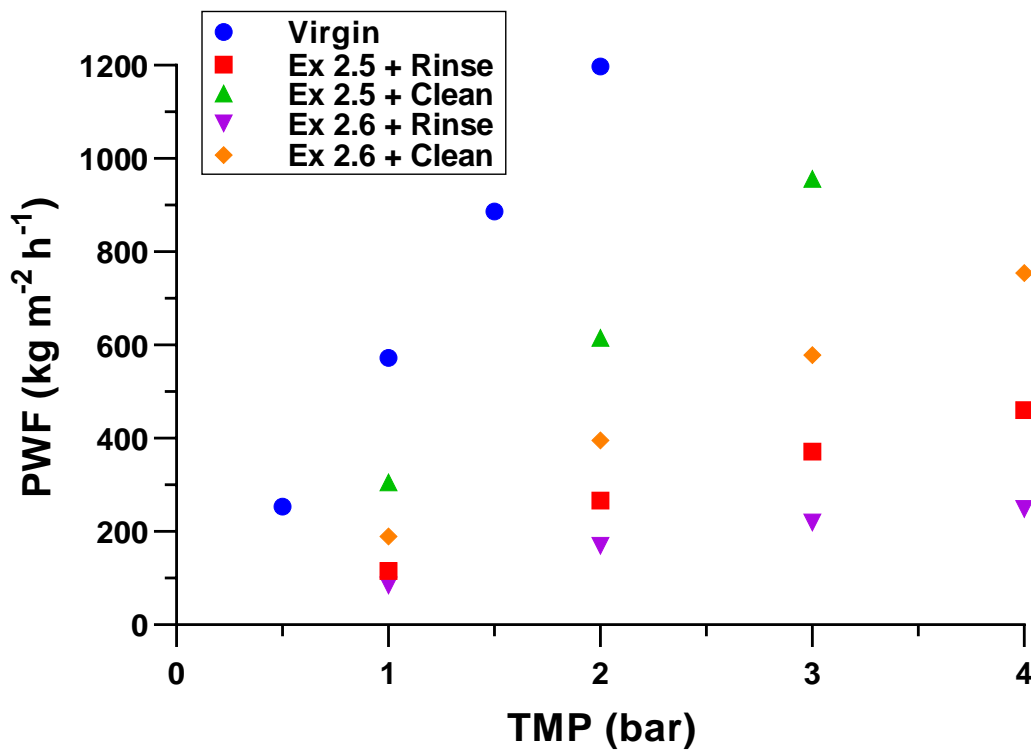


Figure 4.15: PWF vs. TMP of the 150 kD ZrO₂ membrane. The PWF was measured with the unused, cleaned membrane ("virgin"), after filtration and rinsing with water ("+rinse") and after the cleaning cycle ("+clean").

4.5.2 Nanofiltration

PWF during Membrane Screening (Exp. 1.4)

The pure water permeabilities and MgSO_4 rejections measured with each of the virgin membranes (Table 4.9) agreed with the trend expected from their MWCOs and the data from the literature (Table 3.1). The TS80 membrane proved to be the most consistent in terms of resistance to fouling and chemical cleaning, demonstrating very little change in PWF and MgSO_4 retention over the two filtration and cleaning cycles (Figure 4.16). The small flux decline due to fouling for the TS80 ($\sim 12\%$) was made up of approximately equal parts of reversible and irreversible fouling. The PWF of the virgin NP030 membrane was not able to be completely recovered, dropping after the first filtration to $\sim 70\%$ of the original value, though a further, appreciable decrease was not seen after the second filtration. As with the TS80, the decline due to fouling for the NP30 consisted of reversible and irreversible fouling in approximately equal measure.

The PWF data for the ETNA01 membrane did not demonstrate the consistency seen in the other two membranes. For this membrane, the flux increased at almost every stage in the cycle and the MgSO_4 retention dropped steadily from 25.2 to 23.0 to 21.9%. Such behaviour has been observed with many NF membranes and suggests deterioration due to the process conditions and the cleaning regime (135, 136). The occurrence of this performance decline can be the result of many factors, such as pore swelling and defunctionalisation of the membrane surface, and represents a major challenge in process design with polymeric membranes. It is, therefore, essential that membrane screening includes not only flux and retention studies with the target substrate but also a consideration of the cleaning regime and long-term durability of the membrane. In this case, the results of the PWF measurements support the selection of the TS80 as the optimal membrane in this study.

Table 4.9: A comparison of the average pure water permeability and MgSO_4 retention for the nanofiltration (NF) membranes ETNA01, NP030 and TS80 over the course of the two membrane screening experiments (TMP 10-40, 40°C, CFV = 1.1 m s⁻¹)

| Experiment | Permeability ($\text{kg h}^{-1} \text{m}^{-2} \text{bar}^{-1}$) | | | | | MgSO ₄ |
|------------|---|---------|----------|---------|----------|-------------------|
| | Original | + Rinse | Recovery | + Clean | Recovery | Retention |
| | | | % | | % | % |
| ETNA (a) | 9.87 | 10.97 | 111.12 | 13.33 | 135.04 | 23.0 |
| ETNA (b) | 13.33 | 10.52 | 78.89 | 14.54 | 109.06 | 21.9 |
| NP030 (a) | 4.31 | 1.77 | 41.01 | 2.97 | 68.79 | 42.1 |
| NP030 (b) | 2.97 | 1.64 | 55.22 | 3.22 | 108.39 | 41.3 |
| TS80 (a) | 4.01 | 3.52 | 87.82 | 3.82 | 95.50 | 98.0 |
| TS80 (b) | 3.82 | 3.57 | 93.39 | 3.37 | 88.13 | 98.1 |

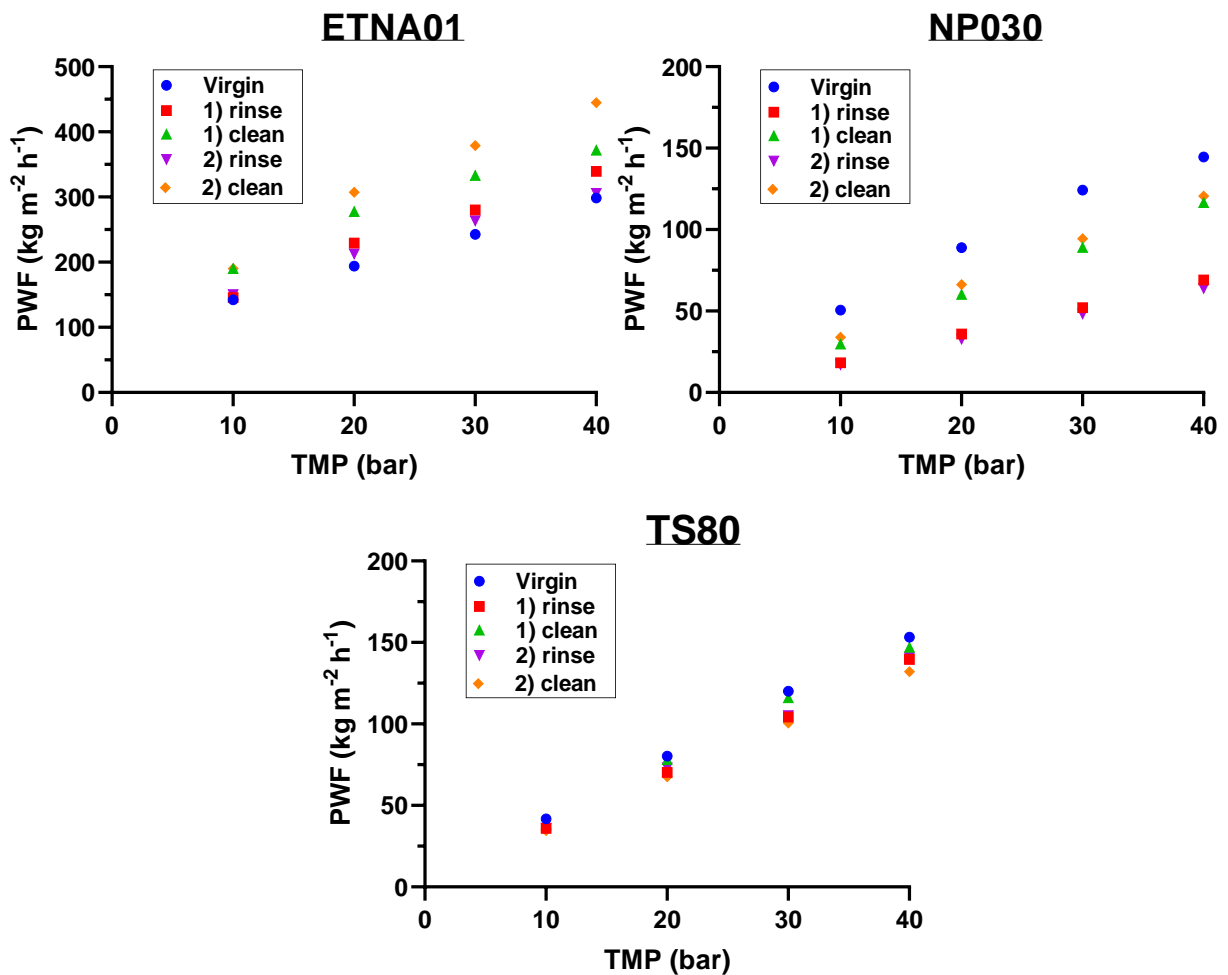


Figure 4.16: A comparison of the PWF of the NF membranes ETNA01, NP030 and TS80 over two filtration and cleaning cycles

TS80 Concentration Experiments (Exp. 2.7/8/9/10 & 3.1)

In comparison to the screening experiments, which were operated in total recirculation mode, the concentration experiments were expected to result in increased levels of membrane fouling. Indeed, the average permeability recovery after cleaning was slightly less (85.4% vs. 91.8%) and resulted in a gradual drop in PWF over the course of the experiments (Table 4.10, Figure 4.17). During the second cleaning cycle, the membrane ruptured. This was first apparent from the excessive permeability in the PWF data and was confirmed by the very low (47.0%) MgSO_4 retention. Both membranes behaved similarly, though their PWF patterns over the filtration cycles were not as consistent and displayed much more variability compared to the screening experiments. Overall, however, the average fouling contributions to PWF decline were similar to Exp. 1.4, comprising almost equally of reversible and irreversible fouling.

Table 4.10: The pure water permeability, flux recovery, fouling contributions and MgSO_4 retention for the nanofiltration (NF) membrane TS80 over the five concentration experiments (TMP 10-40, 40°C, CFV = 1.1 m s⁻¹)

| Exp. | Permeability (kg h ⁻¹ m ⁻² bar ⁻¹) | | | | | % Decline from Fouling | | MgSO ₄ Retention |
|------|--|---------|----------|---------|----------|------------------------|-------|-----------------------------|
| | Original | + Rinse | Recovery | + Clean | Recovery | Irrev. | Rev. | % |
| | | | % | | % | % | % | % |
| 2.7 | 5.55 | 4.19 | 75.43 | 4.53 | 81.69 | 18.31 | 15.01 | 95.9 |
| 2.8 | 4.53 | 2.53 | 55.73 | 4.27 | 94.09 | 5.91 | 38.36 | 91.0 |
| 2.9 | 4.27 | 3.40 | 79.82 | 7.44 | 174.38 | RUPTURED | | 47.0 |
| 2.10 | 4.83 | 3.19 | 66.07 | 3.69 | 76.50 | 23.50 | 10.43 | 99.0 |
| 3.1 | 3.69 | 2.873 | 77.81 | 22.19 | 89.13 | 10.87 | 11.32 | 95.0 |

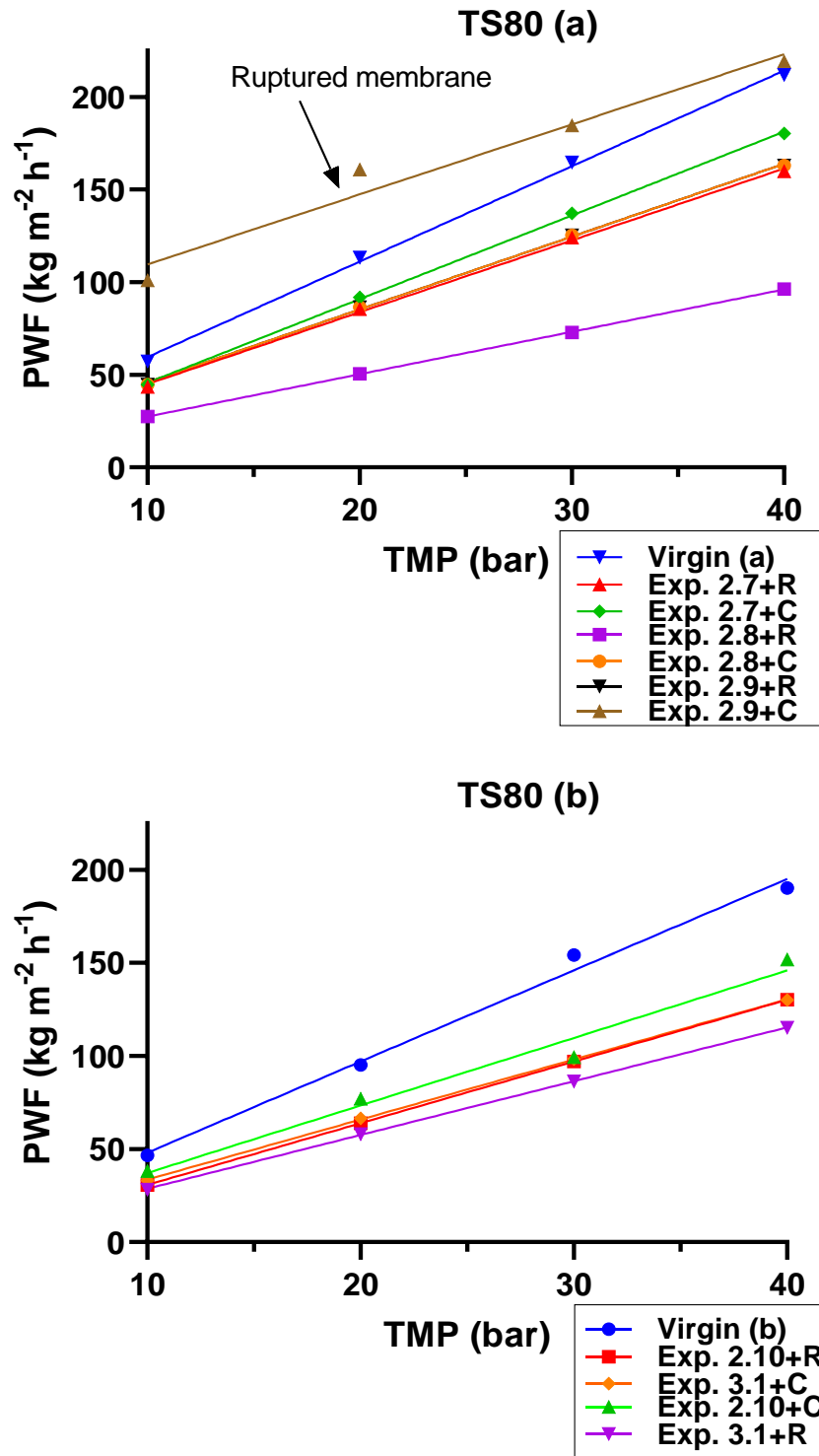


Figure 4.17: The pure water flux (PWF) curves for the two TS80 membranes over the concentration experiments (R = water rinse, C = chemical cleaning) (TMP 10-40, 40°C, CFV = 1.1 m s⁻¹)

Possible Foulants Observed

After the refrigerated storage of the UF permeate, a brown, crystalline precipitate formed (Figure 4.18). Following the NF, a green-brown residue was observed in the feed tank, and after storage of the NF retentate, an oily, white precipitate formed. The crystals could originate from the salts which are added during the fermentation as a nitrogen supplement (urea) and for pH control (NaOH), though their concentrations are likely insufficient for precipitation. Another possibility is that the crystals are formed from struvite ($\text{MgNH}_4\text{PO}_4 \cdot 6\text{H}_2\text{O}$), which can be found in relatively large quantities in FB ($>2 \text{ g L}^{-1}$) and has been shown to be a major foulant in membrane bio-reactors (137). Struvite can be identified by microscopy and ion-chromatography, and it has been shown to be possible to inhibit its formation by the selective removal of NH_4^+ from the FB with combined dialysis and zeolite absorption (138).

The green-brown residue found in the feed tank and seen on the NF membrane surface consists possibly of humic substances which are produced from the microbial degradation of the maize feedstock. Humic substances are known to cause fouling in NF and RO (139, 102) and from the MW (500-10,000 Da) and colour (yellow-brown) ranges, it is likely that many fulvic acids and humic acids pass through the UF and are retained by the NF membrane in this process (140).



Figure 4.18: Photographs of the precipitates and residues found in the NF filtration streams. From left to right: the clear-brown crystalline precipitate from the UF permeate, the green-brown residue from the NF feed tank, and the oily, white precipitate in the NF retentate.

While the determination of low MW humic substances can be achieved by chromatography and spectroscopy, their removal by pretreatment would be more difficult. Precipitation by acidification is possible (141), though it is expensive and

could lead a reduction in MCFA yield as both classes of compounds are poorly soluble at low pH. Removal of humic acids has also been demonstrated by coagulation with aluminium sulphate (142), absorption on activated carbon (143) and lime (144), though this would also add to process costs and could decrease MCFA yields.

Given their large MW, it could be possible to exclude these substances from the NF feed by using a tighter UF membrane, though would likely be at the cost of decreased flux in the UF process. While thermal pretreatment can denature polysaccharide and protein foulants, low MW humic substances are much more stable (145) and their in situ degradation would likely require enzymatic or microbial action (146). Though complicated, this could possibly be achieved by incorporating additional bacteria or fungi to the mixed culture used in the MCCE process, and a more thorough fermentation would certainly improve efficiency in the downstream processes.

5. Conclusion and Outlook

In this study, a separation cascade was developed for the recovery of MCFAs from maize silage FB on a technical scale using the membrane filtration technologies UF and NF.

The first stage in the cascade was a solid-liquid separation with a cloth-lined basket press. The basket press allowed for an average liquid recovery of 82% and decreased the dry residue of the filtrate from 6.7% to 2.4% w/w. The dry residue of the filter cake was, however, only 18% which constitutes a product loss of around 20%. To improve the recovery of this step and validate scalability, trials should be conducted with alternative equipment such as a plate-and-frame filter press or a screw extrusion press, though the product loss in this step is likely not critical to the feasibility of the process. Since MCFAs are a valuable livestock feed additive, the cost of unrecovered product could be recouped by marketing the filter cake to the agricultural industry.

The second stage of the cascade was the removal of suspended solids and organic macromolecules by UF using a ZrO₂ tubular ceramic membrane. Preliminary experiments found that suitable process conditions were a TMP of 3 bar, a temperature of 40°C, and a CFV of 1.7 m s⁻¹. UF of the FB was shown to have negligible retention of MCFAs and to be feasible with quantities exceeding 100 kg over more than 10 hours. Permeate fluxes of around 50 kg m⁻² h⁻¹ were relatively stable until VR > 0.7 and final VRs of around 0.9 were achieved. Filtrations were performed with both untreated and thermally treated FB on 15 kDa and 150 kDa membranes, though very little difference in permeate flux was observed. It is believed that the formation of a cake layer at the membrane surface is the flux limiting factor and it is suggested that this be confirmed by comparing the experimental data to theoretical flux decline models (89, 147). It is further recommended that the UF be attempted with tighter membranes of the same type (1 kDa & 5 kDa) to find the point at which the molecular weight cut-off of the membrane itself is the flux limiting factor.

The third stage of the cascade was the concentration of the MCFAs by NF. The three NF membranes ETNA01PP (Alfa Laval), NP030 (Microdyn Nadir), and TS80 (TriSep) were screened for permeate flux, MCFA retention, and fouling resistance. The Trisep TS80 membrane was found to have the highest performance, whereby it retained more than 90% of C4-C8 FAs and had a steady-state flux of $56 \text{ kg m}^{-2} \text{ h}^{-1}$ at a TMP of 30 bar. Of the four pretreatment combinations, the thermally treated 15 kDa UF permeate was found to have the highest permeate flux in the concentration experiments, though the differences were not substantial. In each case, flux decline was immediate and linear, and at a VR of approximately 0.5, permeate flux had decreased to $<10 \text{ kg m}^{-2} \text{ h}^{-1}$. The final VRs were between 0.55 and 0.65, which corresponds to an approximately two-fold enrichment of MCFAs in the NF retentate. Further concentration of the products was precluded by fouling of the NF membrane.

The flux decline in NF caused by membrane fouling is the most significant problem in the separation cascade as it reduces the efficiency of the process and makes the recovery of the products from the retentate more costly. Two possible types of membrane foulants were isolated and preliminary observations suggest that they could be humic substances and the inorganic salt struvite. Identification of these foulants is recommended before any further process development is considered.

After the foulants have been identified, experiments should be performed to attempt to remove them from the NF feed by pretreatment. This pretreatment could include enzymatic digestion, electrolysis, or using a tighter UF membrane or including an additional filtration step through which the MCFAs pass before being concentrated in the final stage. Of these options, an adaption of the NF/RO membrane combination would be preferable as it would be less expensive. If the foulants can be removed, the process developed in this study could then be optimised and upscaled for use in a biorefinery. If the foulants cannot be removed, and concentration is restricted, the focus should be given to alternative techniques to recover the products from the NF retentate, such as distillation, extraction and adsorption processes.

Future studies should include a broader screening process to identify NF membranes which have similarly high retention the TS80 but have higher permeate fluxes and better fouling resistance. Additionally, it is suggested that experiments are conducted to adapt the standard cleaning regime to the specific substrate-membrane combination. By improving the cleaning process, membrane performance could be more completely recovered after each filtration and more easily maintained over its lifetime.

Although the filtration cascade developed in this study was not able to produce a directly marketable MCFA product, the process shows promise. As it stands, the NF retentate is enriched in C2-C8 FAs by a factor of around two and, aside from the possible membrane foulants, is particle- and macromolecule-free. The product of this membrane cascade can thus provide an improved feedstock for other recovery processes, such as distillation and extraction, which are also currently under development. Either through integration, or ideally, by improvement of the cascade itself, it is believed that the process developed in this thesis has the potential to provide a more cost-effective and environmentally friendly source of MCFAs that can be easily integrated into a biorefinery.

6. References

1. Steffen, W.; Rockström, J.; Richardson, K.; Lenton, T. M.; Folke, C.; Liverman, D.; Summerhayes, C. P.; Barnosky, A. D.; Cornell, S. E.; Crucifix, M.; Donges, J. F.; Fetzer, I.; Lade, S. J.; Scheffer, M.; Winkelmann, R.; Schellnhuber, H. J. Trajectories of the Earth System in the Anthropocene. *Proceedings of the National Academy of Sciences of the United States of America [Online]* **2018**, *115* (33), 8252–8259.
2. Dietz, T.; Börner, J.; Förster, J.; Braun, J. von. Governance of the Bioeconomy: A Global Comparative Study of National Bioeconomy Strategies. *Sustainability [Online]* **2018**, *10* (9), 3190.
3. Scarlat, N.; Dallemand, J.-F.; Monforti-Ferrario, F.; Nita, V. The role of biomass and bioenergy in a future bioeconomy: Policies and facts. *Environmental Development [Online]* **2015**, *15*, 3–34.
4. The German Federal Government. German Biorefinery Roadmap: Biorefineries Roadmap as part of the German Federal Government action plans for the material and energetic utilisation of renewable raw materials. <http://www.bmel.de/SharedDocs/Downloads/Broschueren/RoadmapBioraffinerien.html> (accessed March 31, 2020).
5. International Energy Agency. IEA Bioenergy Country Reports. <https://www.ieabioenergy.com/iea-publications/country-reports/2018-country-reports/> (accessed March 30, 2020).
6. US Government: Biomass Research and Development Technical Advisory Committee. *Roadmap for Bioenergy and Biobased Products in the United State*, 2007.
7. Sariatli, F. Linear Economy Versus Circular Economy: A Comparative and Analyzer Study for Optimization of Economy for Sustainability. *Visegrad Journal on Bioeconomy and Sustainable Development [Online]* **2017**, *6* (1), 31–34.
8. Kamm, B. Biorefineries – their scenarios and challenges. *Pure and Applied Chemistry [Online]* **2014**, *86* (5), 821–831.

9. Schieb, P.-A.; Lescieux-Katir, H.; Thénnot, M.; Clément-Larosi re, B. *Biorefinery 2030*; Springer Berlin Heidelberg: Berlin, Heidelberg, 2015.
10. Bastidas-Oyanedel, J.-R.; Schmidt, J. E. *Biorefinery*; Springer International Publishing: Cham, 2019.
11. Liguori, R.; Faraco, V. Biological processes for advancing lignocellulosic waste biorefinery by advocating circular economy. *Bioresource technology [Online]* **2016**, *215*, 13–20.
12. Umweltbundesamt; KLU. Position Paper: On the Future of Biogas Generation. https://www.umweltbundesamt.de/sites/default/files/medien/376/publikationen/on_the_future_of_biogas_generation_and_utilisation_klu.pdf (accessed May 5, 2020).
13. Witsch, K. Lower Energy: As subsidies are phased out, biogas farmers fight to survive. <https://www.handelsblatt.com/today/companies/lower-energy-as-subsidies-are-phased-out-biogas-farmers-fight-to-survive/23733946.html?ticket=ST-2846926-fgxdUsu1EVLiZWCVXBN-ap4> (accessed May 5, 2020).
14. Theuerl, S.; Herrmann, C.; Heiermann, M.; Grundmann, P.; Landwehr, N.; Kreidenweis, U.; Prochnow, A. The Future Agricultural Biogas Plant in Germany: A Vision. *Energies [Online]* **2019**, *12* (3), 396.
15. Braune M., Daniel-Gromke J., Str uber H. *Von der Biogasanlage zur modernen Bioraffinerie. Conference Paper: 11. Rostocker Bioenergieforum*, 2017. https://www.researchgate.net/publication/319878182_Von_der_Biogasanlage_zur_modernen_Bioraffinerie/link/5b35caada6fdcc8506db742e/download (accessed June 2, 2020).
16. Wu, Q.; Bao, X.; Guo, W.; Wang, B.; Li, Y.; Luo, H.; Wang, H.; Ren, N. Medium chain carboxylic acids production from waste biomass: Current advances and perspectives. *Biotechnology advances [Online]* **2019**, *37* (5), 599–615.
17. Kim, H.; Choi, O.; Jeon, B. S.; Choe, W.-S.; Sang, B.-I. Impact of feedstocks and downstream processing technologies on the economics of caproic acid production in fermentation by *Megasphaera elsdenii* T81. *Bioresource technology [Online]* **2020**, *301*, 122794.

18. Chwialkowska, J.; Duber, A.; Zagrodnik, R.; Walkiewicz, F.; Łężyk, M.; Oleskowicz-Popiel, P. Caproic acid production from acid whey via open culture fermentation - Evaluation of the role of electron donors and downstream processing. *Bioresource technology [Online]* **2019**, 279, 74–83.
19. *Separation and purification technologies in biorefineries*; Ramaswamy, S., Ramarao, B. V., Huang, H.-J., Eds.; Wiley John Wiley & Sons Ltd: Chichester, West Sussex, United Kingdom, 2013.
20. Kohli, K.; Prajapati, R.; Sharma, B. Bio-Based Chemicals from Renewable Biomass for Integrated Biorefineries. *Energies [Online]* **2019**, 12 (2), 233.
21. Moscoviz, R.; Trably, E.; Bernet, N.; Carrère, H. The environmental biorefinery: state-of-the-art on the production of hydrogen and value-added biomolecules in mixed-culture fermentation. *Green Chem. [Online]* **2018**, 20 (14), 3159–3179.
22. Qureshi, N.; Hodge, D. B.; Vertes, A. A. *Biorefineries. Integrated biochemical processes for liquid biofuels*; Elsevier: Amsterdam, 2014.
23. Abels, C.; Carstensen, F.; Wessling, M. Membrane processes in biorefinery applications. *Journal of Membrane Science [Online]* **2013**, 444, 285–317.
24. Koschuh, W.; THANG, V.; Krasteva, S.; Novalin, S.; Kulbe, K. Flux and retention behaviour of nanofiltration and fine ultrafiltration membranes in filtrating juice from a green biorefinery: A membrane screening. *Journal of Membrane Science [Online]* **2005**, 261 (1-2), 121–128.
25. Aghapour Aktij, S.; Zirehpour, A.; Mollahosseini, A.; Taherzadeh, M. J.; Tiraferri, A.; Rahimpour, A. Feasibility of membrane processes for the recovery and purification of bio-based volatile fatty acids: A comprehensive review. *Journal of Industrial and Engineering Chemistry [Online]* **2020**, 81, 24–40.
26. Hu, Y.; Scarborough, M.; Aguirre-Villegas, H.; Larson, R. A.; Noguera, D. R.; Zavala, V. M. A Supply Chain Framework for the Analysis of the Recovery of Biogas and Fatty Acids from Organic Waste. *ACS Sustainable Chem. Eng. [Online]* **2018**, 6 (5), 6211–6222.

27. *Separation processes in the food and biotechnology industries. Principles and applications*; Grandison, A. S., Lewis, M. J., Eds.; Woodhead Pub: Cambridge, England, 1996.
28. Kochkodan, V.; Johnson, D. J.; Hilal, N. Polymeric membranes: surface modification for minimizing (bio)colloidal fouling. *Advances in colloid and interface science [Online]* **2014**, *206*, 116–140.
29. Wainaina, S.; Parchami, M.; Mahboubi, A.; Horváth, I. S.; Taherzadeh, M. J. Food waste-derived volatile fatty acids platform using an immersed membrane bioreactor. *Bioresource technology [Online]* **2019**, *274*, 329–334.
30. Ravi, P. P.; Merkle, W.; Tuczinski, M.; Saravia, F.; Horn, H.; Lemmer, A. Integration of membrane filtration in two-stage anaerobic digestion system: Specific methane yield potentials of hydrolysate and permeate. *Bioresource technology [Online]* **2019**, *275*, 138–144.
31. Angenent, L. T.; Richter, H.; Buckel, W.; Spirito, C. M.; Steinbusch, K. J. J.; Plugge, C. M.; Strik, D. P. B. T. B.; Grootsholten, T. I. M.; Buisman, C. J. N.; Hamelers, H. V. M. Chain Elongation with Reactor Microbiomes: Open-Culture Biotechnology To Produce Biochemicals. *Environmental science & technology [Online]* **2016**, *50* (6), 2796–2810.
32. Harvey, B. G.; Meylemans, H. A. 1-Hexene: A renewable C6 platform for full-performance jet and diesel fuels. *Green Chem [Online]* **2014**, *16* (2), 770–776.
33. Urban, C.; Xu, J.; Sträuber, H.; dos Santos Dantas, T. R.; Mühlenberg, J.; Härtig, C.; Angenent, L. T.; Harnisch, F. Production of drop-in fuels from biomass at high selectivity by combined microbial and electrochemical conversion. *Energy Environ. Sci. [Online]* **2017**, *10* (10), 2231–2244.
34. Earth Energy Renewables. Production of High Value Chemicals From Low Value Biodegradable Materials. https://www.iowabio.org/documents/filelibrary/images/iba_events/pfg_2017/Earth_Energy_Renewables_501D04B83E4F3.pdf (accessed March 3, 2020).
35. Dai, K.; Zhang, W.; Zeng, R. J.; Zhang, F. Production of chemicals in thermophilic mixed culture fermentation: mechanism and strategy. *Critical Reviews in Environmental Science and Technology [Online]* **2020**, *50* (1), 1–30.

36. Sauer, M.; Porro, D.; Mattanovich, D.; Branduardi, P. Microbial production of organic acids: Expanding the markets. *Trends in biotechnology [Online]* **2008**, 26 (2), 100–108.
37. Scarborough, M. J.; Lynch, G.; Dickson, M.; McGee, M.; Donohue, T. J.; Noguera, D. R. Increasing the economic value of lignocellulosic stillage through medium-chain fatty acid production. *Biotechnology for biofuels [Online]* **2018**, 11, 200.
38. *Carboxylic acid production*; Lidén, G., Ed., First edition; MDPI: Basel, Beijing, Wuhan, Barcelona, Belgrade, 2017.
39. Dwidar, M.; Park, J.-Y.; Mitchell, R. J.; Sang, B.-I. The future of butyric acid in industry. *The Scientific World Journal [Online]* **2012**, 2012, 471417.
40. Zigová, J.; Šturdík, E. Advances in biotechnological production of butyric acid. *J Ind Microbiol Biotech [Online]* **2000**, 24 (3), 153–160.
41. *Industrial crops. Breeding for bioenergy and bioproducts*; Cruz, V. M. V., Dierig, D. A., Eds.; Handbook of plant breeding 9; Springer: New York, Heidelberg, Dordrecht, London, 2015.
42. *Edible oil and fat products. Chemistry, properties, and health effects*; Shahidi, F., Ed., 6. ed.; Bailey's industrial oil & fat products Vol. 1; Wiley-Interscience: New York, 2005.
43. Gervajio, G. C.; Withana-Gamage, T. S.; Sivakumar, M. Fatty Acids and Derivatives from Coconut Oil. In *Bailey's industrial oil and fat products*, 6th; Shahidi, F., Bailey, A. E., Eds.; Wiley-Interscience: New York, Chichester, 2005; pp 1–45.
44. Bloemhof-Ruwaard, J. M.; Koudijs, H. G.; Vis, J. C. Environmental impacts of fat blends. *Environ Resource Econ [Online]* **1995**, 6 (4), 371–387.
45. Mikkola, J.-P.; Sklavounos, E.; King, A. W. T.; Virtanen, P. The Biorefinery and Green Chemistry. In *Ionic Liquids in the Biorefinery Concept*; Bogel-Lukasik, R., Ed.; Green Chemistry Series; Royal Society of Chemistry: Cambridge, 2015; pp 1–37.
46. Chen, W.-S.; Strik, D. P. B. T. B.; Buisman, C. J. N.; Kroeze, C. Production of Caproic Acid from Mixed Organic Waste: An Environmental Life Cycle

- Perspective. *Environmental science & technology [Online]* **2017**, 51 (12), 7159–7168.
47. *Mixed Culture Chain Elongation (MCCE)—A Novel Biotechnology for Renewable Biochemical Production from Organic Residual Streams. Energy Engineering*; Raghavan, K. V., Ghosh, P., Chen, W. S., Roghair, M., Triana Mecerreyes, D., Strik, D. P. B. T. B., Kroeze, C., Buisman, C. J. N., Eds.; Springer Singapore, 2017.
 48. Agler, M. T.; Spirito, C. M.; Usack, J. G.; Werner, J. J.; Angenent, L. T. Chain elongation with reactor microbiomes: Upgrading dilute ethanol to medium-chain carboxylates. *Energy Environ. Sci. [Online]* **2012**, 5 (8), 8189.
 49. Cavalcante, W. d. A.; Leitão, R. C.; Gehring, T. A.; Angenent, L. T.; Santaella, S. T. Anaerobic fermentation for n-caproic acid production: A review. *Process Biochemistry [Online]* **2017**, 54, 106–119.
 50. Zhu, X.; Tao, Y.; Liang, C.; Li, X.; Wei, N.; Zhang, W.; Zhou, Y.; Yang, Y.; Bo, T. The synthesis of n-caproate from lactate: a new efficient process for medium-chain carboxylates production. *Scientific reports [Online]* **2015**, 5, 14360.
 51. Lambrecht, J.; Cichocki, N.; Schattenberg, F.; Kleinstaub, S.; Harms, H.; Müller, S.; Sträuber, H. Key sub-community dynamics of medium-chain carboxylate production. *Microbial cell factories [Online]* **2019**, 18 (1), 92.
 52. Sarria, S.; Kruyer, N. S.; Peralta-Yahya, P. Microbial synthesis of medium-chain chemicals from renewables. *Nature biotechnology [Online]* **2017**, 35 (12), 1158–1166.
 53. Roghair, M.; Liu, Y.; Strik, D. P. B. T. B.; Weusthuis, R. A.; Bruins, M. E.; Buisman, C. J. N. Development of an Effective Chain Elongation Process From Acidified Food Waste and Ethanol Into n-Caproate. *Frontiers in bioengineering and biotechnology [Online]* **2018**, 6, 50.
 54. Jeon, B. S.; Kim, B.-C.; Um, Y.; Sang, B.-I. Production of hexanoic acid from D-galactitol by a newly isolated *Clostridium* sp. BS-1. *Applied microbiology and biotechnology [Online]* **2010**, 88 (5), 1161–1167.

55. Han, W.; He, P.; Shao, L.; Lü, F. Road to full bioconversion of biowaste to biochemicals centering on chain elongation: A mini review. *Journal of environmental sciences (China) [Online]* **2019**, *86*, 50–64.
56. Ge, S.; Usack, J. G.; Spirito, C. M.; Angenent, L. T. Long-Term n-Caproic Acid Production from Yeast-Fermentation Beer in an Anaerobic Bioreactor with Continuous Product Extraction. *Environmental science & technology [Online]* **2015**, *49* (13), 8012–8021.
57. Cavalcante, W. A.; Gehring, T. A.; Santaella, S. T.; Freitas, I. B.F.; Angenent, L. T.; van Haandel, A. C.; Leitão, R. C. Upgrading sugarcane biorefineries: Acetate addition allows for conversion of fermented sugarcane molasses into high-value medium chain carboxylic acids. *Journal of Environmental Chemical Engineering [Online]* **2020**, *8* (2), 103649.
58. Chaincraft B.V. Chaincraft: Biobased Innovators. <https://www.chaincraft.nl/> (accessed February 29, 2020).
59. Ricci, A.; Allende, A.; Bolton, D.; Chemaly, M.; Davies, R.; Herman, L.; Koutsoumanis, K.; Lindqvist, R.; Nørrung, B.; Robertson, L.; Ru, G.; Sanaa, M.; Simmons, M.; Skandamis, P.; Snary, E.; Speybroeck, N.; Kuile, B. T.; Threlfall, J.; Wahlström, H.; Girones, R.; Alvarez Ordoñez, A.; Griffin, J.; Correia, S.; Fernández Escámez, P. Evaluation of the application for a new alternative processing method for animal by-products of Category 3 material (ChainCraft B.V.). *EFS2 [Online]* **2018**, *16* (6), 264.
60. Sträuber, H.; Bühligen, F.; Kleinstüber, S.; Dittrich-Zechendorf, M. Carboxylic acid production from ensiled crops in anaerobic solid-state fermentation - trace elements as pH controlling agents support microbial chain elongation with lactic acid. *Eng. Life Sci. [Online]* **2018**, *18* (7), 447–458.
61. Wasewar, K. L.; Shende, D. Z. Reactive Extraction of Caproic Acid Using Tri- n - butyl Phosphate in Hexanol, Octanol, and Decanol. *J. Chem. Eng. Data [Online]* **2011**, *56* (2), 288–297.
62. Wang, Y.; Li, Y.; Li, Y.; Wang, J.; Li, Z.; Dai, Y. Extraction Equilibria of Monocarboxylic Acids with Trialkylphosphine Oxide. *J. Chem. Eng. Data [Online]* **2001**, *46* (4), 831–837.

63. Jeon, B. S.; Moon, C.; Kim, B.-C.; Kim, H.; Um, Y.; Sang, B.-I. In situ extractive fermentation for the production of hexanoic acid from galactitol by *Clostridium* sp. BS-1. *Enzyme and microbial technology* [Online] **2013**, 53 (3), 143–151.
64. Wasewar, K. L.; Shende, D. Z. Extraction of Caproic Acid Using Tri- n -butyl Phosphate in Benzene and Toluene at 301 K. *J. Chem. Eng. Data* [Online] **2010**, 55 (9), 4121–4125.
65. Kucek, L. A.; Spirito, C. M.; Angenent, L. T. High n-caprylate productivities and specificities from dilute ethanol and acetate: Chain elongation with microbiomes to upgrade products from syngas fermentation. *Energy Environ. Sci.* [Online] **2016**, 9 (11), 3482–3494.
66. Kucek, L. A.; Nguyen, M.; Angenent, L. T. Conversion of L-lactate into n-caproate by a continuously fed reactor microbiome. *Water research* [Online] **2016**, 93, 163–171.
67. Xu, J.; Guzman, J. J. L.; Andersen, S. J.; Rabaey, K.; Angenent, L. T. In-line and selective phase separation of medium-chain carboxylic acids using membrane electrolysis. *Chemical Communications* [Online] **2015**, 51 (31), 6847–6850.
68. *Membrane technologies for biorefining*; Figoli, A., Cassano, A., Basile, A. B., Eds.; Woodhead Publishing series in energy no. 96; Woodhead Publishing; Elsevier, 2016.
69. Khunnonkwao, P.; Jantama, K.; Kanchanatawee, S.; Galier, S.; Roux-de Balman, H. A two steps membrane process for the recovery of succinic acid from fermentation broth. *Separation and Purification Technology* [Online] **2018**, 207, 451–460.
70. Lee, H. D.; Lee, M. Y.; Hwang, Y. S.; Cho, Y. H.; Kim, H. W.; Park, H. B. Separation and Purification of Lactic Acid from Fermentation Broth Using Membrane-Integrated Separation Processes. *Ind. Eng. Chem. Res.* [Online] **2017**, 56 (29), 8301–8310.
71. González, M. I.; Alvarez, S.; Riera, F. A.; Álvarez, R. Lactic acid recovery from whey ultrafiltrate fermentation broths and artificial solutions by nanofiltration. *Desalination* [Online] **2008**, 228 (1-3), 84–96.

72. *Bioprocessing of renewable resources to commodity bioproducts*; Bisaria, V. S., Kondō, A., Eds.; Wiley: Hoboken New Jersey, 2014.
73. McKinlay, J. B.; Vieille, C.; Zeikus, J. G. Prospects for a bio-based succinate industry. *Applied microbiology and biotechnology* [Online] **2007**, 76 (4), 727–740.
74. López-Garzón, C. S.; Straathof, A. J. J. Recovery of carboxylic acids produced by fermentation. *Biotechnology advances* [Online] **2014**, 32 (5), 873–904.
75. Zacharof, M.-P.; Mandale, S. J.; Williams, P. M.; Lovitt, R. W. Nanofiltration of treated digested agricultural wastewater for recovery of carboxylic acids. *Journal of Cleaner Production* [Online] **2016**, 112, 4749–4761.
76. Atasoy, M.; Owusu-Agyeman, I.; Plaza, E.; Cetecioglu, Z. Bio-based volatile fatty acid production and recovery from waste streams: Current status and future challenges. *Bioresource technology* [Online] **2018**, 268, 773–786.
77. Jänisch, T.; Reinhardt, S.; Pohsner, U.; Böringer, S.; Bolduan, R.; Steinbrenner, J.; Oechsner, H. Separation of volatile fatty acids from biogas plant hydrolysates. *Separation and Purification Technology* [Online] **2019**, 223, 264–273.
78. Bellona, C.; Drewes, J. E. The role of membrane surface charge and solute physico-chemical properties in the rejection of organic acids by NF membranes. *Journal of Membrane Science* [Online] **2005**, 249 (1-2), 227–234.
79. Bøddiker, K. W. *Liquid separations with membranes. An introduction to barrier interference*; Springer: Berlin, Heidelberg, 2008.
80. Strathmann, H. Membrane separation processes: Current relevance and future opportunities. *AIChE J.* [Online] **2001**, 47 (5), 1077–1087.
81. Strathmann, H. *Introduction to membrane science and technology*; Wiley-VCH: Weinheim, 2011.
82. Baker, R. W. *Membrane technology and applications*, 2. ed., reprinted.; Wiley: Chichester, 2008.
83. *Basic Equations of the Mass Transport through a Membrane Layer*; Nagy, E., Ed.; Elsevier, 2012.

84. Abdelrasoul, A.; Doan, H.; Lohi, A.; Cheng, C.-H. Mass Transfer Mechanisms and Transport Resistances in Membrane Separation Process. In *Mass Transfer - Advancement in Process Modelling*; Solecki, M., Ed.; InTech, 2015.
85. Nagy, E. On Mass Transport Through a Membrane Layer. In *Basic Equations of the Mass Transport through a Membrane Layer*; Nagy, E., Ed.; Elsevier, 2012; pp 1–34.
86. Tu, N. P. Role of Charge Effects during Membrane Filtration. Master's, University of Gent, 2013.
87. Mullett, M.; Fornarelli, R.; Ralph, D. Nanofiltration of Mine Water: Impact of Feed pH and Membrane Charge on Resource Recovery and Water Discharge. *Membranes [Online]* **2014**, 4 (2), 163–180.
88. Doran, P. M. *Bioprocess engineering principles, second edition*, 2nd ed.; Academic Press: Waltham, Mass., 2013.
89. Di Bella, G.; Di Trapani, D. A Brief Review on the Resistance-in-Series Model in Membrane Bioreactors (MBRs). *Membranes* **2019**, 9 (2). DOI: 10.3390/membranes9020024.
90. Hilal, N.; Ogunbiyi, O. O.; Miles, N. J.; Nigmatullin, R. Methods Employed for Control of Fouling in MF and UF Membranes: A Comprehensive Review. *Separation Science and Technology [Online]* **2005**, 40 (10), 1957–2005.
91. Thamaraiselvan, C.; Noel, M. Membrane Processes for Dye Wastewater Treatment: Recent Progress in Fouling Control. *Critical Reviews in Environmental Science and Technology [Online]* **2015**, 45 (10), 1007–1040.
92. Križan Milić, J.; Murić, A.; Petrinić, I.; Simonić, M. Recent Developments in Membrane Treatment of Spent Cutting-Oils: A Review. *Ind. Eng. Chem. Res. [Online]* **2013**, 52 (23), 7603–7616.
93. Judd, S. Membrane technology. *Membranes for Industrial Wastewater Recovery and Re-use*; Elsevier, 2003; pp 13–74.
94. Vrijen Hoek, E. M.; Tarabara, V. V. *Encyclopedia of membrane science and technology*; Wiley: Hoboken, New Jersey, 2013.

95. Li X., L. J. Critical Flux. In *Encyclopedia of Membranes*; Drioli, E., Giorno, L., Eds.; Springer Berlin Heidelberg; Imprint: Springer: Berlin, Heidelberg, 2019.
96. Bacchin, P. Critical and sustainable fluxes: Theory, experiments and applications. *Journal of Membrane Science [Online]* **2006**, *281* (1-2), 42–69.
97. Di Trapani, D.; Di Bella, G.; Mannina, G.; Torregrossa, M.; Viviani, G. Effect of C/N shock variation on the performances of a moving bed membrane bioreactor. *Bioresource technology [Online]* **2015**, *189*, 250–257.
98. Deng, L.; Guo, W.; Ngo, H. H.; Zhang, J.; Liang, S.; Xia, S.; Zhang, Z.; Li, J. A comparison study on membrane fouling in a sponge-submerged membrane bioreactor and a conventional membrane bioreactor. *Bioresource technology [Online]* **2014**, *165*, 69–74.
99. Sun, J.; Xiao, K.; Mo, Y.; Liang, P.; Shen, Y.; Zhu, N.; Huang, X. Seasonal characteristics of supernatant organics and its effect on membrane fouling in a full-scale membrane bioreactor. *Journal of Membrane Science [Online]* **2014**, *453*, 168–174.
100. Wu, B.; Kitade, T.; Chong, T. H.; Uemura, T.; Fane, A. G. Role of initially formed cake layers on limiting membrane fouling in membrane bioreactors. *Bioresource technology [Online]* **2012**, *118*, 589–593.
101. Zhang, M.; Peng, W.; Chen, J.; He, Y.; Ding, L.; Wang, A.; Lin, H.; Hong, H.; Zhang, Y.; Yu, H. A new insight into membrane fouling mechanism in submerged membrane bioreactor: osmotic pressure during cake layer filtration. *Water research [Online]* **2013**, *47* (8), 2777–2786.
102. Amy, G. Fundamental understanding of organic matter fouling of membranes. *Desalination [Online]* **2008**, *231* (1-3), 44–51.
103. Taniguchi, M.; Kilduff, J. E.; Belfort, G. Low fouling synthetic membranes by UV-assisted graft polymerization: monomer selection to mitigate fouling by natural organic matter. *Journal of Membrane Science [Online]* **2003**, *222* (1-2), 59–70.
104. Purkait, M. K.; Singh, R. *Membrane technology in separation science*; Taylor & Francis: Boca Raton, 2018.

105. Bokhary, A.; Tikka, A.; Leitch, M.; Liao, B. Membrane Fouling Prevention and Control Strategies in Pulp and Paper Industry Applications: A Review. *Journal of Membrane Science and Research [Online]* **2018**, 4 (4), 181–197.
106. Dvořák, L.; Gómez, M.; Dvořáková, M.; Růžicková, I.; Wanner, J. The impact of different operating conditions on membrane fouling and EPS production. *Bioresource technology [Online]* **2011**, 102 (13), 6870–6875.
107. Kasmi, M.; Hamdi, M.; Trabelsi, I. Processed milk waste recycling via thermal pretreatment and lactic acid bacteria fermentation. *Environmental science and pollution research international [Online]* **2017**, 24 (15), 13604–13613.
108. Porcelli, N.; Judd, S. Chemical cleaning of potable water membranes: A review. *Separation and Purification Technology [Online]* **2010**, 71 (2), 137–143.
109. atech innovations gmbh. Technical Data of atech Al₂O₃ membranes. https://www.atech-innovations.com/fileadmin/downloads/atech_innovations_product_data_en.pdf (accessed December 3, 2019).
110. Microdyn Nadir. Trisep TS80. <https://www.microdyn-nadir.com/wp-content/uploads/TS80.pdf> (accessed February 27, 2020).
111. Microdyn Nadir. NP030. <https://www.microdyn-nadir.com/wp-content/uploads/NP030-P-Flat-Sheet-Membrane.pdf> (accessed February 28, 2020).
112. Alfa Laval. Alfa Laval UF flat sheet membranes. https://www.alfalaval.com/globalassets/documents/products/separation/membranes/flat-sheet-membranes/uf-flat-sheet-membranes_200000311-1-en-gb.pdf (accessed January 27, 2020).
113. Gautam, A.; Menkhaus, T. J. Performance evaluation and fouling analysis for reverse osmosis and nanofiltration membranes during processing of lignocellulosic biomass hydrolysate. *Journal of Membrane Science [Online]* **2014**, 451, 252–265.
114. Tundis, R.; Loizzo, M. R.; Bonesi, M.; Sicari, V.; Ursino, C.; Manfredi, I.; Conidi, C.; Figoli, A.; Cassano, A. Concentration of Bioactive Compounds from Elderberry (*Sambucus nigra* L.) Juice by Nanofiltration Membranes. *Plant foods for human nutrition (Dordrecht, Netherlands) [Online]* **2018**, 73 (4), 336–343.

115. Verliefde, A. R. D. *Rejection of organic micropollutants by high pressure membranes (NF)*; Water Management Academic Press: Delft, 2008.
116. Vieira, G. S.; Moreira, F. K.V.; Matsumoto, R. L.S.; Michelon, M.; Filho, F. M.; Hubinger, M. D. Influence of nanofiltration membrane features on enrichment of jussara ethanolic extract (*Euterpe edulis*) in anthocyanins. *Journal of Food Engineering [Online]* **2018**, 226, 31–41.
117. Harrison, C.; Le Gouellec, Y.; Cheng, R.; Childress, A. Bench-Scale Testing of Nanofiltration for Seawater Desalination. *Journal of Environmental Engineering* **2007**, 133.
118. Nghiem, L. Removal of emerging trace organic contaminants by nanofiltration and reverse osmosis. PhD; University of Wollongong, Australia, 2005.
119. Niewersch, C.; Koh, C. N.; Wintgens, T.; Melin, T.; Schaum, C.; Cornel, P. Potentials of using nanofiltration to recover phosphorus from sewage sludge. *Water science and technology : a journal of the International Association on Water Pollution Research [Online]* **2008**, 57 (5), 707–714.
120. Giacobbo, A.; Bernardes, A. M.; Pinho, M. N. de. Nanofiltration for the Recovery of Low Molecular Weight Polysaccharides and Polyphenols from Winery Effluents. *Separation Science and Technology [Online]* **2013**, 48 (17), 2524–2530.
121. Streit, K. F.; Ferreira, J. Z.; Bernardes, A. M.; Norberta De Pinho, M. Ultrafiltration/nanofiltration for the tertiary treatment of leather industry effluents. *Environmental science & technology [Online]* **2009**, 43 (24), 9130–9135.
122. Persson, T.; Jönsson, A.-S. Fouling of Ultrafiltration Membranes during Isolation of Hemicelluloses in the Forest Industry. *Scholarly Research Exchange [Online]* **2009**, 2009 (11), 1–7.
123. Khairul Zaman, N.; Jeng Yih, L.; Pui Vun, C.; Rohani, R.; Mohammad, A. W. Recovery of Organic Acids from Fermentation Broth Using Nanofiltration Technologies: A Review. *JPS [Online]* **2017**, 28 (Suppl. 1), 85–109.

124. International Organization for Standardization. *DIN ISO 15705:2003-01, Wasserbeschaffenheit_ - Bestimmung des chemischen Sauerstoffbedarfs (ST-CSB)_ - Küvettentest (ISO_15705:2002)*; Beuth Verlag GmbH: Berlin, 2003.
125. DIN - Deutsches Institut für Normung e. V. *DIN EN 12880:2001-02, Charakterisierung von Schlämmen - Bestimmung des Trockenrückstandes und des Wassergehalts; Deutsche Fassung EN_12880:2000*; Beuth Verlag GmbH: Berlin, 2001.
126. Perlmutter, B. A. *Solid-liquid filtration. Practical guides in chemical engineering*; Elsevier: Amsterdam, 2015.
127. Tarleton, E. S.; Wakeman, R. J. *Solid. Equipment selection and process design / E.S. Tarleton, R.J. Wakeman*; Butterworth-Heinemann: Oxford, 2007.
128. Fitriani; Sekiguchi, M.; Kokugan, T. Separation and Concentration of Lactate from Cassava Fermentation Broth by Reverse Osmosis. *Membranes [Online]* **2010**, 35 (5), 248–256.
129. Morão, A.; Britesalves, A.; Geraldles, V. Concentration polarization in a reverse osmosis/nanofiltration plate-and-frame membrane module. *Journal of Membrane Science [Online]* **2008**, 325 (2), 580–591.
130. Liew, M.K.H.; Tanaka, S.; Morita, M. Separation and purification of lactic acid: Fundamental studies on the reverse osmosis down-stream process. *Desalination [Online]* **1995**, 101 (3), 269–277.
131. Aouni, A.; Fersi, C.; Cuartas-Urbe, B.; Bes-Pía, A.; Alcaina-Miranda, M. I.; Dhahbi, M. Reactive dyes rejection and textile effluent treatment study using ultrafiltration and nanofiltration processes. *Desalination [Online]* **2012**, 297, 87–96.
132. Waeger, F.; Delhay, T.; Fuchs, W. The use of ceramic microfiltration and ultrafiltration membranes for particle removal from anaerobic digester effluents. *Separation and Purification Technology [Online]* **2010**, 73 (2), 271–278.
133. Luo, J.; Cao, W.; Ding, L.; Zhu, Z.; Wan, Y.; Jaffrin, M. Y. Treatment of dairy effluent by shear-enhanced membrane filtration: The role of foulants.

- Separation and Purification Technology [Online]* **2012**, 96, 194–203 (accessed April 20, 2020).
134. Law J. Y., Mohammad A. W. Separation of Succinate from Organic Acid Salts Using Nanofiltration Membrane. *Chemical Engineering Transactions [Online]* **2017**, 56, 1705–1710 (accessed April 21, 2020).
 135. Al-Amoudi, A.; Lovitt, R. W. Fouling strategies and the cleaning system of NF membranes and factors affecting cleaning efficiency. *Journal of Membrane Science [Online]* **2007**, 303 (1-2), 4–28.
 136. Wadekar, S. S.; Wang, Y.; Lokare, O. R.; Vidic, R. D. Influence of Chemical Cleaning on Physicochemical Characteristics and Ion Rejection by Thin Film Composite Nanofiltration Membranes. *Environmental science & technology [Online]* **2019**, 53 (17), 10166–10176.
 137. Yoon, S. H.; Kang, I. J.; Lee, C. H. Fouling of Inorganic Membrane and Flux Enhancement in Membrane-Coupled Anaerobic Bioreactor. *Separation Science and Technology [Online]* **1999**, 34 (5), 709–724 (accessed April 20, 2020).
 138. Kim, J.; Lee, C.-H.; Choo, K.-H. Control of struvite precipitation by selective removal of NH_4^+ with dialyzer/zeolite in an anaerobic membrane bioreactor. *Applied microbiology and biotechnology [Online]* **2007**, 75 (1), 187–193.
 139. Lin, C.-F.; Yu-Chen Lin, A.; Sri Chandana, P.; Tsai, C.-Y. Effects of mass retention of dissolved organic matter and membrane pore size on membrane fouling and flux decline. *Water research [Online]* **2009**, 43 (2), 389–394 (accessed April 20, 2020).
 140. Perminova, I. V.; Frimmel, F. H.; Kudryavtsev, A. V.; Kulikova, N. A.; Abbt-Braun, G.; Hesse, S.; Petrosyant, V. S. Molecular weight characteristics of humic substances from different environments as determined by size exclusion chromatography and their statistical evaluation. *Environmental science & technology [Online]* **2003**, 37 (11), 2477–2485.
 141. Zeng, W.; Xu, S.; Du, G.; Liu, S.; Zhou, J. Separation and purification of α -ketoglutarate and pyruvate from the fermentation broth of *Yarrowia lipolytica*. *Bioprocess and biosystems engineering [Online]* **2018**, 41 (10), 1519–1527.

142. Vik, E. A.; Eikebrokk, B. Coagulation Process for Removal of Humic Substances from Drinking Water. In *Aquatic humic substances: Influence on fate and treatment of pollutants / I.H. Suffet, editor, Patrick MacCarthy, editor; Suffet, I. H., MacCarthy, P., Eds.; Advances in chemistry series 219; American Chemical Society: Washington, D.C., 1989; pp 385–408.*
143. Edwards, G. A.; Amirtharajah, A. Removing Color Caused by Humic Acids. *Journal - American Water Works Association [Online]* **1985**, 77 (3), 50–57.
144. Liao, M. Y.; Randtke, S. J. Removing Fulvic Acid by Lime Softening. *Journal - American Water Works Association [Online]* **1985**, 77 (8), 78–88.
145. Sonnenberg, L. B.; Johnson, J. D.; Christman, R. F. Chemical Degradation of Humic Substances for Structural Characterization. In *Aquatic humic substances: Influence on fate and treatment of pollutants / I.H. Suffet, editor, Patrick MacCarthy, editor; Suffet, I. H., MacCarthy, P., Eds.; Advances in chemistry series 219; American Chemical Society: Washington, D.C., 1989; pp 3–23.*
146. Gramss; Ziegenhagen; Sorge. Degradation of Soil Humic Extract by Wood- and Soil-Associated Fungi, Bacteria, and Commercial Enzymes. *Microbial ecology [Online]* **1999**, 37 (2), 140–151.
147. Vincent Vela, M. C.; Álvarez Blanco, S.; Lora García, J.; Bergantiños Rodríguez, E. Analysis of membrane pore blocking models adapted to crossflow ultrafiltration in the ultrafiltration of PEG. *Chemical Engineering Journal [Online]* **2009**, 149 (1-3), 232–241.

7. Appendices

7.1 Physical and Chemical Data of the Filtration Streams

Table 7.1: Physical and chemical data of each stream in the study

| Experiment | Stream | pH | Electrical Conductivity | Dry Residue | COD | Density |
|------------|-----------|-------|----------------------------|----------------|-------------|--------------|
| | | | $mS\ cm^{-1}$ | % w/w | $g\ L^{-1}$ | $g\ mL^{-1}$ |
| Exp. 1.1 | Permeate | 7.10 | 23.9 | 2.49 | - | - |
| | Retentate | - | - | 22.95 | - | - |
| Exp. 1.2 | Heating | 8.30 | 23.3 | 2.43 | - | - |
| Exp. 1.3 | Permeate | 8.08 | 23.7 | 2.30 | - | - |
| | Retentate | 8.06 | 22.7 | 8.13 | - | - |
| Exp. 1.4 | TS80 | 9.04 | 14.02 | 0.06 | - | - |
| | Permeate | | | | | |
| | NP030 | 10.00 | 1.43 | 1.14 | - | - |
| | Permeate | | | | | |
| | ETNA | 8.83 | 17.75 | 1.52 | - | - |
| | Permeate | | | | | |
| Exp. 2.1 | Filtrate | 6.69 | 21.3 | 1.95 | 60.2 | 1.008 |
| | Retentate | - | - | 18.49 | 0.0 | - |
| Exp. 2.2 | Heating | 7.11 | 21.0 | 1.75 | 53.7 | 1.007 |
| Exp. 2.3 | Permeate | 7.24 | 21.4 | 1.99 | 40.6 | 1.008 |
| | Retentate | 7.22 | 20.0 | 5.27 | 121.1 | 1.020 |
| Exp. 2.4 | Permeate | 6.80 | 22.7 | 1.59 | 42.6 | 1.008 |
| | Retentate | 6.97 | 19.7 | 5.43 | 123.2 | 1.021 |
| Exp. 2.5 | Permeate | 7.14 | 20.9 | 2.20 | 44.5 | 1.008 |
| | Retentate | 7.22 | 19.5 | 5.00 | 108.0 | 1.017 |
| Exp. 2.6 | Permeate | 6.96 | 21.7 | 1.70 | 45.6 | 1.008 |
| | Retentate | 7.14 | 19.7 | 4.70 | 121.1 | 1.016 |
| Exp. 2.7 | Permeate | 9.70 | 5.0 | 0.19 | 6.8 | 0.998 |
| | Retentate | 8.92 | 44.5 | 4.71 | 108.0 | 1.019 |
| Exp. 2.8 | Permeate | 9.80 | 3.3 | 0.10 | - | 1.000 |
| | Retentate | 9.60 | 37.9 | 3.52 | - | 1.017 |
| Exp. 2.9 | Permeate | 9.70 | 3.9 | 0.16 | - | 1.000 |
| | Retentate | 9.10 | 40.6 | 4.37 | - | 1.020 |
| Exp. 2.10 | Permeate | 10.20 | 4.3 | 0.16 | - | - |
| | Retentate | 9.70 | 41.9 | 4.20 | - | - |
| Exp. 3.1 | Permeate | - | | | | |
| | Retentate | - | | | | |

Table 7.2: Fatty Acid (FA) (C2-C8) concentration for each stream in the study

| Fatty Acid Concentration (g L⁻¹) | | | | |
|--|-------|------|------|------|
| Experiment (stream) | C2 | C4 | C6 | C8 |
| Exp. 1.1 Basket Press | 9.83 | 3.48 | 3.64 | 0.51 |
| Exp. 1.2 Heating | 10.31 | 3.70 | 3.92 | 0.57 |
| Exp. 1.3 Permeate | 10.51 | 3.61 | 3.91 | 0.58 |
| Exp. 1.3 Retentate | 10.36 | 3.24 | 3.97 | 0.67 |
| Exp. 2.1 | 9.32 | 2.92 | 2.35 | 0.34 |
| Exp. 2.2 | 8.91 | 2.83 | 2.22 | 0.30 |
| Exp. 2.3 Permeate | 8.90 | 2.71 | 2.17 | 0.30 |
| Exp. 2.3 Retentate | 8.81 | 2.82 | 2.26 | 0.32 |
| Exp. 2.4 Permeate | 8.98 | 2.74 | 2.26 | 0.32 |
| Exp. 2.4 Retentate | 9.68 | 3.06 | 2.33 | 0.35 |
| Exp. 2.5 Permeate | 9.07 | 2.78 | 2.22 | 0.31 |
| Exp. 2.5 Retentate | 9.46 | 2.97 | 2.38 | 0.34 |
| Exp. 2.6 Permeate | 8.68 | 2.70 | 2.19 | 0.31 |
| Exp. 2.6 Retentate | 9.40 | 2.99 | 2.29 | 0.34 |
| Exp. 2.7 Permeate | 1.32 | 0.21 | 0.17 | 0.03 |
| Exp. 2.7 Retentate | 24.14 | 7.60 | 5.94 | 0.81 |
| Exp. 2.8 Permeate | 0.96 | 0.17 | 0.15 | 0.03 |
| Exp. 2.8 Retentate | 19.23 | 5.85 | 4.72 | 0.67 |
| Exp. 2.9 Permeate | 1.20 | 0.21 | 0.18 | 0.03 |
| Exp. 2.9 Retentate | 21.69 | 6.76 | 5.29 | 0.72 |
| Exp. 2.10 Permeate | 1.31 | 0.21 | 0.19 | 0.04 |
| Exp. 2.10 Retentate | 22.55 | 6.90 | 5.62 | 0.79 |
| Exp. 3.1 Permeate | 3.72 | 0.48 | 0.45 | 0.06 |
| Exp. 3.1 Retentate | 22.28 | 6.08 | 5.83 | 0.67 |
| Exp. 3.2 | 19.30 | 5.22 | 5.07 | 0.57 |

7.2 Ultrafiltration

Table 7.3: Rejection coefficients with respect to the C2-C8 fatty acids for the ultrafiltration concentration experiments (Exp. 1.3 & 2.3-2.6)

| Fatty Acid Retention | | | | |
|----------------------|--------|-------|--------|--------|
| Experiment | C2 | C4 | C6 | C8 |
| 1.3: 15 kD heated | -0.018 | 0.023 | 0.001 | -0.015 |
| 2.3: 15 kD heated | 0.001 | 0.045 | 0.022 | 0.020 |
| 2.4: 15 kD | 0.036 | 0.062 | 0.039 | 0.057 |
| 2.5: 150 kD heated | -0.019 | 0.019 | -0.003 | -0.010 |
| 2.6: 150 kD | 0.025 | 0.047 | 0.010 | -0.024 |

7.3 Nanofiltration

Table 7.4: Rejection coefficients with respect to the C2-C8 fatty acids for the NF membranes ETNA01, NP030, and TS80

| Ethanoic Acid Retention | | | |
|-------------------------|-------|-------|-------|
| <i>pressure (bar)</i> | 20 | 30 | 40 |
| ETNA01 | 0.295 | 0.330 | 0.319 |
| NP030 | 0.397 | 0.499 | 0.545 |
| TS80 | 0.922 | 0.966 | 0.970 |

| Butanoic Acid Retention | | | |
|-------------------------|-------|-------|-------|
| <i>pressure (bar)</i> | 20 | 30 | 40 |
| ETNA01 | 0.291 | 0.330 | 0.321 |
| NP030 | 0.474 | 0.564 | 0.597 |
| TS80 | 0.948 | 0.977 | 0.979 |

| Hexanoic Acid Retention | | | |
|-------------------------|-------|-------|-------|
| <i>pressure (bar)</i> | 20 | 30 | 40 |
| ETNA01 | 0.222 | 0.251 | 0.244 |
| NP030 | 0.515 | 0.593 | 0.621 |
| TS80 | 0.949 | 0.979 | 0.980 |

| Octanoic Acid Retention | | | |
|-------------------------|-------|-------|-------|
| <i>pressure (bar)</i> | 20 | 30 | 40 |
| ETNA01 | 0.137 | 0.159 | 0.161 |
| NP030 | 0.572 | 0.631 | 0.652 |
| TS80 | 0.950 | 0.978 | 0.980 |